

**PART VI:**

# WFPC2

---

**Chapter 24: WFPC2 Instrument Overview**

**Chapter 25: WFPC2 Data Structures**

**Chapter 26: WFPC2 Calibration**

**Chapter 27: WFPC2 Error Sources**

**Chapter 28: WFPC2 Data Analysis**

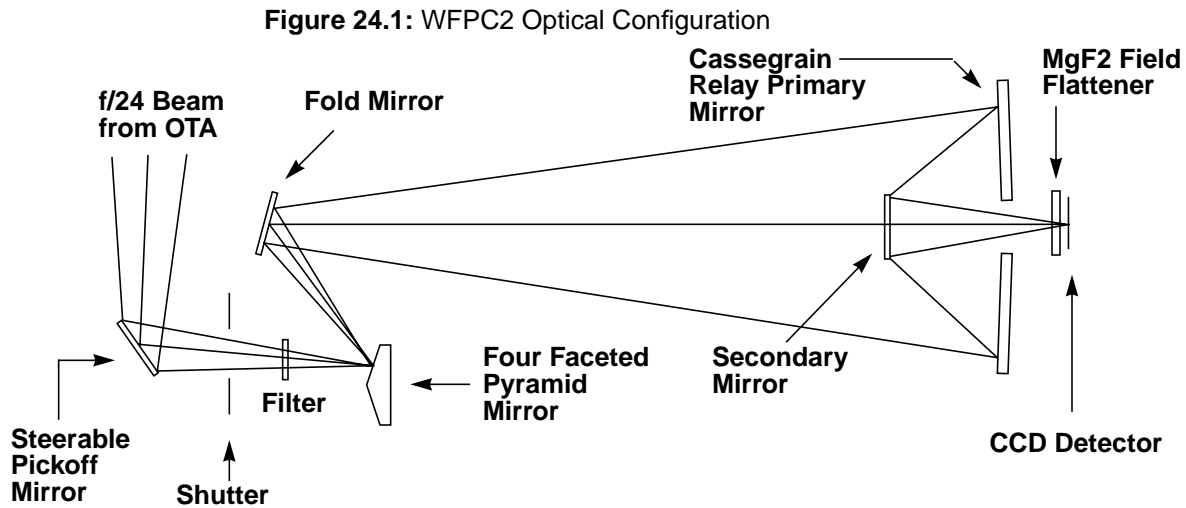
■ WFPC2

# WFPC2 Instrument Overview

The Wide Field and Planetary Camera 2 (WFPC2) is a two-dimensional imaging device covering a wavelength range from Lyman- $\alpha$  to about 1  $\mu\text{m}$ . It was built at the Jet Propulsion Laboratory by an Investigation Definition Team (IDT) headed by John Trauger, as a replacement for the first Wide Field and Planetary Camera (WF/PC). WFPC2 includes built-in correction for the spherical aberration of the HST Optical Telescope Assembly (OTA). The WFPC2 was installed in HST during the First Servicing Mission in December 1993. An early IDT report of the WFPC2 on-orbit performance can be found in Trauger et al. (1994, *ApJ*, 435, L3), and a more detailed assessment of its capabilities in Holtzman et al. (1995, *PASP*, 107, page 156 and page 1065).

The WFPC2 field of view is located at the center of the HST focal plane; Figure 24.1 shows a schematic of its optical arrangement. The central portion of the  $f/24$  beam coming from the OTA is intercepted by a steerable pick-off mirror attached to the WFPC2 and is diverted through an open port entry into the WFPC2. The beam then passes through a shutter and interposable filters. A total of 48 spectral elements and polarizers are contained in an assembly of 12 filter wheels. The light then falls onto a shallow-angle, four-faceted pyramid located at the aberrated OTA focus. Each face of the pyramid is a concave spherical surface. The pyramid divides the OTA image of the sky into four parts. After leaving the pyramid, each quarter of the full field of view is relayed by an optical flat to a Cassegrain relay that forms a second field image on a charge-coupled device (CCD) of 800 x 800 pixels. Each of these four detectors is housed in a cell sealed by a  $\text{MgF}_2$  window. This window is figured to serve as a field flattener.

The aberrated HST wavefront is corrected by introducing an equal but opposite error in each of the four Cassegrain relays. An image of the HST primary mirror is formed on the secondary mirrors in the Cassegrain relays. The spherical aberration from the telescope's primary mirror is corrected on these secondary mirrors, which are extremely aspheric; the resulting point spread function is quite close to that originally expected for WF/PC-1.



The optics of three of the four cameras are essentially identical and produce a final focal ratio of  $f/12.9$ . These are the Wide Field Cameras (WF2, WF3, WF4). The fourth camera, known as the Planetary Camera (PC or PC1), has a focal ratio of  $f/28.3$ .

Figure 24.2 shows the field of view of WFPC2 projected on the sky. The readout direction is marked with arrows near the start of the first row in each CCD. The  $x,y$  coordinate directions are for POS-TARG commands. The position angle of V3 on the sky varies with pointing direction and observation epoch and is given in the calibrated science header by the keyword PA\_V3.

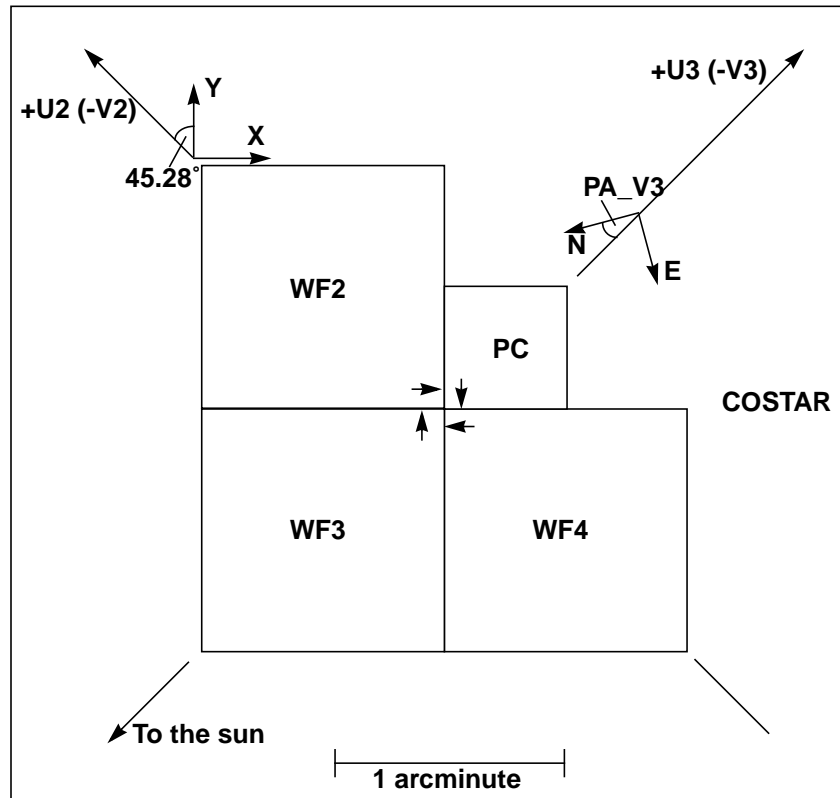
**Table 24.1: Camera Configurations**

Camera	Pixels	Field of View	Scale	f/ratio
PC	800 x 800	36" x 36"	0.0455" per pixel	28.3
WF2, 3, 4	800 x 800	80" x 80"	0.0996" per pixel	12.9

The Planetary Camera (PC) provides a field of view sufficient to obtain full disk images of all planets except for Jupiter. However, even with this high resolution camera, the pixels undersample the point spread function of the telescope and camera optics by a factor of two at 5800 Å. The WF pixels are over a factor of two larger, and thus undersample the image by a factor of four at visual wavelengths. It is possible to recover some of the sampling lost to these large pixels by image dithering, i.e., taking observations at different sub-pixel offsets. A short discussion of dithering is provided in “Dithering” on page 28-19.

Two readout modes are available on the WFPC2: FULL and AREA (the mode used for a given observation is shown in the MODE keyword in the image header). In FULL mode each pixel is read out individually. In AREA mode pixels

**Figure 24.2:** WFPC2 Field of View Projected on the Sky



are summed in 2 x 2 boxes before readout. The advantage of the AREA mode is that readout noise for the larger pixels is nearly the same as for the unsummed pixels:  $6e^-$  vs.  $5e^-$  per pixel. Thus, AREA mode can be useful in observations of extended sources when readout is the primary source of noise (often the case in the far UV).

The readout direction of the four CCDs is defined such that in IRAF pixel numbering (origin at lower left corner), the origin of the CCD lies at the corner of the chip pointing towards the center of the WFPC2 pyramid (see Figure 24.2). As a result of the aberration of the primary beam, the light from sources near the pyramid edges is divided between adjacent chips, and consequently the lower columns and rows of the PC and WF chips are strongly vignetted, as shown in Table 24.2. The CCD  $x,y$  (column,row) numbers given in this table vary at the 1–2 pixel level because of bending and tilting of the field edge in detector coordinates due to geometric distortion in the camera. The orientation of each camera on the

sky is provided by the `ORIENTAT` group keyword in the image headers. The geometry of the cameras and the related keywords are explained in greater detail in Chapter 25.

**Table 24.2:** Inner Field Edges of Field Projected Onto CCDs

Camera	Start Vignetted Field	Contiguous Field	Start Unvignetted Field
PC1	$x > 0$ and $y > 8$	$x > 44$ and $y > 52$	$x > 88$ and $y > 96$
WF2	$x > 26$ and $y > 6$	$x > 46$ and $y > 26$	$x > 66$ and $y > 46$
WF3	$x > 10$ and $y > 27$	$x > 30$ and $y > 47$	$x > 50$ and $y > 67$
WF4	$x > 23$ and $y > 24$	$x > 43$ and $y > 44$	$x > 63$ and $y > 64$

A quick way of putting an image together from its four chips is provided by the STSDAS task `wmosaic`, which can also be used for WF/PC-1 images. This task, in its default mode, will combine the four chips in a large, 1600 x 1600 pixel image at the resolution of the Wide Field cameras, resampling the pixels in order to correct for the chip overlap, rotations, and distortions. Of course, resolution will be lost in the PC, whose pixels are rebinned to the resolution of the Wide Field Cameras (a factor 2.3 coarser). The images produced by `wmosaic` are usually quite adequate for presentations and the identification of interesting features, but are not recommended for science uses because of the loss of resolution and photometric accuracy associated with data resampling, especially in the PC.

# WFPC2 Data Structures

## In This Chapter...

Data Files and Suffixes / 25-1

Header Keywords / 25-3

Correlating Phase II Exposures with Data Files / 25-8

WFPC2 Paper Products / 25-10

This chapter describes how WFPC2 data are configured and delivered and how these data products relate to the original specifications in the Phase II proposal. We describe the data format used by STScI to distribute WFPC2 data and the meanings of the header keywords that the user is likely to find most important. Finally, we describe the paper products sent to the Principal Investigator (PI) with the initial data delivery and how Archive users can reproduce them.

---

## 25.1 Data Files and Suffixes

HST data files are generally distributed in FITS format, either via tape or electronically from the Archive, and need to be converted into the so-called GEIS format using the STSDAS task **strfits**. Users not familiar with GEIS format or the **strfits** task should consult Chapter 2. After conversion, a directory listing (type `dir` within IRAF) will show that the files all have a nine-character rootname and a three-character suffix (formerly called the “extension”). For each instrument, this suffix uniquely identifies the file contents. The WFPC2 suffixes are listed in Table 25.1.

Files whose suffix ends with the letter “h” (e.g., `u2850303p.c1h`) are ASCII *header files*. The header files contain keywords that describe the parameters used to take the observation, the processing of the data, and the properties of the image. Files whose suffix ends in the letter “d” (e.g., `u2850303p.c1d`) are binary *data files*; these files contain the data as well as the group keywords. A single GEIS image is composed of a header and data *pair* (e.g., the files `u2850303p.c1h` and `u2850303p.c1d` together represent a single image). Note that, in FITS format, header and data are combined into a

single file. For network transfers, the name of the FITS file is composed as follows: *rootname\_suffix.fits*, with the letter “f” replacing “h” or “d” in the suffix (e.g., *u2850303p\_c1f.fits*).

**Table 25.1:** WFPC2 Dataset Suffixes and File Sizes

Suffix	File Contents	Approximate Size
<i>Raw Data Files</i>		
.d0h/ .d0d	Raw science data	5 MB
.q0h/ .q0d	Data quality for raw science data	5 MB
.x0h/ .x0d	Extracted engineering data	100 kB
.q1h/ .q1d	Data quality for extracted engineering data	100 kB
.shh/ .shd	Standard header packet containing observation parameters	30 kB
.pdq	Text file containing jitter statistics and other data quality information	20 kB
<i>Calibrated Data Files</i>		
.c0h/ .c0d	Calibrated science data	10 MB
.c1h/ .c1d	Data quality for calibrated science data	5 MB
.c2h/ .c2d	Histogram of science data pixel values	220 kB
.trl	Trailer file	20 kB

A single WFPC2 exposure is obtained as four images (one image for each CCD chip). GEIS files use group format to keep all of the data from a given HST exposure together in a single image file (see Chapter 2). The data corresponding to each sub-image for the WFPC2 are stored sequentially in the groups of a single GEIS image. The header file for an image contains the information that applies to the observation as a whole (i.e., to all the groups in the image), viewable by paging the header. The group-specific (that is, chip-specific) keyword information is stored with the group data itself in the binary data file; group keywords are only accessible via specialized software, such as the STSDAS tasks **hedit** or **imhead**.

WFPC2 images are normally four-group images: the first group is used for the planetary camera and groups 2, 3, and 4 are used for the wide field cameras. If only a subset of chips are read out, only a subset of groups will be present. The group keyword DETECTOR lists the detector used for that group (1 through 4).

## 25.2 Header Keywords

In Table 25.2 we list those header keywords found in a calibrated WFPC2 image (suffix .c0h) that many observers are likely to find useful. A complete list of header keywords, with brief explanations, can be found in the Keyword Dictionary, available on the STScI Web pages:

<http://archive.stsci.edu/keyword>

The STSDAS tasks **hedit** or **imhead** can be used to view any or all of the header and group keywords. WFPC2 keywords include items such as observing mode, integration time, filters and reference files used, calibration steps performed, and the properties of the data itself (e.g., number of groups, dimensions in pixels of each group, reference pixels, coordinates, scale, flux units, image statistics). Some additional calibration information is given at the end of the header file in HISTORY keywords.

Some keywords can occasionally be confusing. Users should pay special attention to DATE, which refers to the date the file was written, as opposed to DATE-OBS, the date of the observation; FILTER1 and FILTER2, which are the numerical designations of the filter(s) used, while the filter names are FILTNAM1 and FILTNAM2; and PHOTZPT, which is *not* the photometric zeropoint (in the ST magnitude system) as normally understood, but rather the zeropoint in the ST magnitude system to be used after conversion to FLAM units (see “Photometric Zero Point” on page 28-2).

Astrometry keywords can also be confusing. The orientation of the image is specified by a global keyword, PA\_V3, and a group keyword, ORIENTAT. The keyword PA\_V3 gives the position angle (in degrees) of the telescope’s V3 axis on the sky, measured from North through East. The V3 axis is roughly 225 degrees from the  $x$  axis of the PC. This axis differs by exactly 180 degrees from the ORIENT value specified in the Phase II submission, which refers to the U3 axis. The group keyword ORIENTAT gives, for each detector, the position angle of the  $y$  axis in the plane of the sky, measured from North through East. This angle differs from PA\_V3 by roughly  $-135$ ,  $-45$ ,  $+45$ , and  $+135$  degrees, for PC1, WF2, WF3, and WF4, respectively. See Figure 24.2 for a graphic representation of the geometric relationship between the four detectors. Accurate values of the positions and rotations between chips can be obtained from the Science Instrument Aperture File (SIAF). The SIAF is available via the WWW at:

[http://www.stsci.edu/ftp/instrument\\_news/Observatory/siaf.html](http://www.stsci.edu/ftp/instrument_news/Observatory/siaf.html)

In addition, each group has eight keywords (listed under coordinate-related keywords below) that specify the transformation from pixels to world coordinates (right ascension and declination) in the tangent plane approximation at the center of the chip.

**Table 25.2:** WFPC2 Header Keywords

<b>Keyword</b>	<b>Description</b>
<i>Information about the groups</i>	
GROUPS	Multi-group image? Indicates whether data has groups.
GCOUNT	Number of groups per observation (1 to 4)
<i>Coordinate-related keywords</i>	
CRVAL1	RA of reference pixel (deg)
CRVAL2	Dec of reference pixel (deg)
CRPIX1	X coordinate of reference pixel
CRPIX2	Y coordinate of reference pixel
CD1_1	Partial derivative of RA with respect to x
CD1_2	Partial derivative of RA with respect to y
CD2_1	Partial derivative of Dec with respect to x
CD2_2	Partial derivative of Dec with respect to y
<i>Orientation</i>	
MIR_REVR	Is image mirror reversed?
ORIENTAT	Orientation of y axis (deg)—different for each group
<i>Bias level information (columns 3–14 of the .x0h/.x0d file)</i>	
DEZERO	Bias level from engineering data
BIASEVEN	Bias level based on average of odd columns in .x0h/ .x0d file (even columns in science image)
BIASODD	Bias level based on average of even columns in .x0h/ .x0d file (odd columns in science image)
<i>Pixel statistics</i>	
GOODMIN	Minimum value of “good” pixels (not flagged in DQF)
GOODMAX	Maximum value of “good” pixels
DATAMEAN	Mean value of “good” pixels
<i>Photometry keywords</i>	
PHOTMODE	Photometry mode
PHOTFLAM	Inverse sensitivity (units of erg/sec/cm <sup>2</sup> /Å for 1 DN/sec)
PHOTZPT	Zeropoint (currently -21.10, if DOPHOTOM = yes)
PHOTPLAM	Pivot wavelength (in angstroms)
PHOTBW	rms bandwidth of filter (in angstroms)

**Table 25.2:** WFPC2 Header Keywords (Continued)

<b>Keyword</b>	<b>Description</b>
<i>Image statistics keywords</i>	
MEDIAN	Middle data value when good quality pixels sorted
HISTWIDE	Width of the histogram
SKEWNESS	Skewness of the histogram
MEANC10	Mean of a 10 x 10 region at the center of the chip
MEANC100	Mean of a 100 x 100 region at the center of the chip
MEANC300	Mean of a 300 x 300 region at the center of the chip
BACKGRND	Estimated background level
<i>Image keywords</i>	
INSTRUME	Instrument used; always WFPC2
ROOTNAME	Rootname of the observation set
FILETYPE	SHP - standard header packet EXT - extracted engineering file EDQ - EED data quality file SDQ - science data quality file SCI - science data file
MODE	Mode: FULL (full resol.) or AREA (2 x 2 pixel summation)
SERIALS	Serial clocks: ON, OFF
<i>Data type keywords</i>	
IMAGETYP	DARK/BIAS/IFLAT/UFLAT/VFLAT/KSPOT/EXT/ECAL
CDBSFILE	GENERIC/BIAS/DARK/FLAT/MASK/NO Is the image a reference file and if so, type is specified
<i>Reference file selection keywords</i>	
DATE	File creation date (dd/mm/yy)
FILTNAM1	First filter name
FILTNAM2	Second filter name; blank if none
FILTER1	First filter number (0–48) (Historical, but used in SOGS)
FILTER2	Second filter number (0–48)
FILTROT	Partial filter rotation angle (degrees)
<i>More reference file selection keywords</i>	
ATODGAIN	Analog to digital gain (electrons/DN)

**Table 25.2:** WFPC2 Header Keywords (Continued)

<b>Keyword</b>	<b>Description</b>
<i>Calibration switches</i>	
MASKCORR	Do mask correction: PERFORM, OMIT, COMPLETE
ATODCORR	Do A-to-D correction: PERFORM, OMIT, COMPLETE
BLEVCORR	Do bias level correction: PERFORM, OMIT, COMPLETE
BIASCORR	Do bias correction: PERFORM, OMIT, COMPLETE
DARKCORR	Do dark correction: PERFORM, OMIT, COMPLETE
FLATCORR	Do flatfield correction: PERFORM, OMIT, COMPLETE
SHADCORR	Do shaded shutter correction: PERFORM, OMIT, COMPLETE
DOSATMAP	Output saturated pixel map: PERFORM, OMIT, COMPLETE
DOPHOTOM	Fill photometry keywords: PERFORM, OMIT, COMPLETE
DOHISTOS	Make histograms: PERFORM, OMIT, COMPLETE
OUTDTYPE	Output image datatype: REAL, LONG, SHOR—always set to REAL by PODPS pipeline
<i>Calibration reference files used<sup>a</sup></i>	
MASKFILE	Name of the input static mask containing known bad pixels and charge traps
ATODFILE	Name of the A-to-D conversion file
BLEVFILE	Name of engineering file with extended register data
BLEVDFIL	Name of data quality file (DQF) for the engineering file
BIASFILE	Name of the bias frame reference file
BIASDFIL	Name of the bias frame reference DQF
DARKFILE	Name of the dark reference file
DARKDFIL	Name of the dark reference DQF
FLATFILE	Name of the flatfield reference file
FLATDFIL	Name of the flatfield reference DQF
SHADFILE	Name of the reference file for shutter shading
PHOTTAB	Name of the photometry calibration table
SATURATE	Data value at which saturation occurs (always 4095 for WFPC2, which includes the bias)

**Table 25.2:** WFPC2 Header Keywords (Continued)

<b>Keyword</b>	<b>Description</b>
<i>Ephemeris data</i>	
PA_V3	Position angle of V3 axis of HST
RA_SUN	Right ascension of the sun (deg)
DEC_SUN	Declination of the sun (deg)
EQNX_SUN	Equinox of the sun
<i>Fill values</i>	
PODPSFF	0 (no fill), 1 (fill present)
RSDPFILL	Bad data fill value set in pipeline for calibrated image
<i>Exposure Information</i>	
DARKTIME	Estimate of darktime (in sec)
EQUINOX	Equinox of the celestial coordinate system
SUNANGLE	Angle between sun and V1 axis (deg)
MOONANGL	Angle between moon and V1 axis (deg)
SUN_ALT	Altitude of the sun above Earth's limb (deg)
FGSLOCK	Commanded FGS lock (FINE, COARSE, GYROS, UNKNOWN)
<i>Timing information</i>	
DATE-OBS	UT date of start of observation (dd/mm/yy)
TIME-OBS	UT time of start of observation (hh:mm:ss)
EXPSTART	Exposure start time (Modified Julian Date)
EXPEND	Exposure end time (Modified Julian Date)
EXPTIME	Exposure duration (seconds)
EXPFLAG	How exposure time was calculated. (NORMAL, INTERRUPTED, INCOMPLETE, EXTENDED, UNCERTAIN, INDETERMINATE, or PREDICTED)
<i>Proposal information</i>	
TARGNAME	Proposer's target name
RA_TARG	Right ascension of the target (deg) (J2000)
DEC_TARG	Declination of the target (deg) (J2000)
PROPOSID	RPS2 proposal identifier

a. Calibration reference file keywords are populated even if unused.

## 25.3 Correlating Phase II Exposures with Data Files

Because of the need to schedule observations as efficiently as possible, the order in which exposures are executed may be different from the order in which they appear in the observer's Phase II submission—unless an explicit special requirement dictates otherwise. As a result, the data may be received in an order that differs from that originally proposed by the observer. In this section we discuss how to correlate the data received with the exposures specified in the Phase II submission, which can often facilitate the process of interpreting the observations and their interconnection. For archival researchers, recent Phase II specifications submitted by the original observer can be consulted at:

<http://presto.stsci.edu/public/propinfo.html>

The first step is often identifying to which program a data file belongs, which can be accomplished via the header keyword PROPOSID. Data files can then be associated with the corresponding exposure line in the Phase II proposal by comparing exposure information in the Phase II proposal with data file header keywords. For WFPC2 data, the most useful comparisons are shown in the table below.

**Table 25.3:** Comparing Phase II Proposal Keywords to Data Header Keywords

Phase II	Data Header
Target_Name	TARGNAME
Position	RA_TARG, DEC_TARG
Spectral Element	FILTNAME
Time_Per_Exposure	EXPTIME

A convenient tool for viewing some of the most important data header keywords in an easy-to-read formatted output is the STSDAS task **iminfo**. An example of the output of this task is shown in Figure 25.1. Note that the data header keywords are expanded to standard English words in this output. The header file (.c0h extension) can also be examined with IRAF tools **hedit** or **imheader**, with any standard text editor, or simply by listing the contents of the file. Again, please note that a standard text editor will not display the group keywords, which are stored in the image file.

In the specific example shown in Figure 25.1 we see that the Proposal ID is given as 05837. Entering the proposal ID into the space provided on the Web page listed above (without the leading 0) and clicking on **[Get Program Information]**, brings up the Program Information page for that proposal. Under Program Contents on that page you can choose either the file typed in during Phase II or a formatted output. The latter may be easier to read; we reproduce a portion of that file in Figure 25.2.

**Figure 25.1:** Displaying WFPC2 Header Keywords with `iminfo`

```

-----
Rootname          Instrument      Target Name
U2P60204T        WFPC2          CAL-GANY-W

Program           = 2P6          Obs Date        = 19/08/95
Observation set  = 02          Proposal ID     = 05837
Observation      = 04          Exposure ID    = 02-023
Source           = Tape Recorded  Right ascension = 16:16:34.4
File Type        = SCI          Declination    = -20:45:14
Equinox          = J2000

First filtername = F410M          Number of groups = 4
Second filtername =                    Data type       = real

Image type       = EXT          Exposure time (sec) = 5.
Mode             = FULL        Dark time (sec)    = 5.
Serials          = OFF
Shutter          = B
Kelsall spot lamp = OFF        Calibration steps done:
im> █           MASK ATOD BLEV BIAS FLAT SHAD

```

The Exposure ID listed by `iminfo` is 02-023. This corresponds to visit 02, exposure 23. A different format was used in Cycles 0 through 4; exposures in these proposals have a single, unique numeric identifier. To reach this exposure line, page down through the proposal until visit 02 is reached. Now search for exposure 23 in visit 02. As shown in Figure 25.2, this exposure requested a single 5 second exposure of target CAL-GANY-W through filter F410M. A quick comparison with the keywords listed by `iminfo` shows that, indeed, this data file contains the observation specified in this exposure line.

**Figure 25.2:** Exposure Log Sheet for WFPC2

```

Visit: 02
Visit Requirements: BEFORE 16-oct-95
On Hold Comments: <none>
Additional Comments: This visit has limited scheduling opportunities, we prefer as close to
                    Jupiter opposition as possible exp-time calculated from observed Callisto WF
                    images from SL9 campaign

```

Exposure Number	Target Name	Instr Config	Oper. Mode	Aper or F0W	Spectral Element	Central Wavelength	Optional Parameters	Num Exp	Time	Special Requirements
21	cal-gany-w	WFPC2	IMAGE	PC1	F218W		ATD-GAIN=7	2	500s	NO SPLIT
22	cal-gany-w	WFPC2	IMAGE	PC1	F255W		ATD-GAIN=7	1	40s	
23	cal-gany-w	WFPC2	IMAGE	PC1	F410M		ATD-GAIN=15	1	5s	
24	cal-gany-w	WFPC2	IMAGE	PC1	F953H		ATD-GAIN=15	1	30s	
25	cal-gany-w	WFPC2	IMAGE	PC1	F675W		ATD-GAIN=15	1	0.2s	
26	cal-gany-w	WFPC2	IMAGE	PC1	F300W		ATD-GAIN=15	1	10s	

A comparison of these keywords should quickly reveal the data file corresponding to a given exposure line. There are, however, two cases in which such a comparison is somewhat more complicated.

It is recommended that WFPC2 exposures longer than 600 seconds be split into two shorter exposures to facilitate removal of cosmic rays. If the optional

parameters `CR-SPLIT` and `CR-TOLERANCE` are omitted in the Phase II submission, and the exposure *is* longer than 600 seconds, it will be split into two exposures for more efficient scheduling. The default `CR-TOLERANCE` of 0.2 can be used, meaning that the split exposure times could each range from 30–70% of the total exposure, with their sum equal to the original total exposure time.

Exposure times may occasionally be shortened by up to 20% without the approval of the PI, provided that the resulting S/N is 90% of that with the original exposure time. Such changes may be required to fit observations into specific orbital time slots. If, after examining your exposure headers, you still have questions regarding the execution of your observing plan, we recommend you speak with your program's Contact Scientist.

The output generated by `iminfo` contains information on the target, exposure time, and filters used but nothing on guide star status. The `hselect` task, used as follows, provides access to that information by printing the `FGSLOCK` header keyword to the screen:

```
c1> hselect u2p60204t.c0h FGSLOCK yes
FINE
```

The `FGSLOCK` keyword can have the values `FINE`, `COARSE`, `GYROS`, or `UNKNOWN`. Coarse tracking is no longer allowed, so this keyword in recent data will most likely read either `FINE` or `GYROS`. Gyro tracking allows a drift rate of approximately 1 mas/sec. It would only be used if requested by the proposer. `FINE` tracking typically holds pointing with an rms error of less than 7 mas. Typically two guide stars are used in HST observations, but on occasion only one appropriate guide star can be found. Such observations will suffer from small drift rates (a few mas in a 1000 second exposure). If you suspect the quality of tracking obtained during your observations, please review Appendix C which describes how to determine the number and quality of guide stars actually used as well as how to use the OMS jitter files.

---

## 25.4 WFPC2 Paper Products

As part of the initial data delivery, the observer receives a package of so-called *paper products*, which are intended to provide a quick look at the data in hard-copy form. The paper products changed significantly in August 1997; we will describe first their newest version, and then discuss the changes from the previous version. The paper products are generated by the STSDAS task `pp_dads` provided with STSDAS version 2.0. This task enables archival users to generate their own sets of paper products.

The current paper product package consists of two parts. The first is a visit-level overview of the datasets in the package, meant to be similar to the observing log in ground-based observations. The information is presented in three separate tables: Target List, Observation List, and Observation Statistics. The Target List gives the targets observed in this visit, with their positions. The Observation List includes essential information on each dataset, such as rootname,

target name, operating mode, aperture, filter, exposure time, and a number of flags intended to alert the user to any procedural problem with the data. The flags are represented graphically by circles, open when the data are okay, filled if any (potential) problem is encountered, to be detailed in the second part. The Observation Statistics is a table with basic image statistics for each dataset, such as mean counts, background level, and a rough estimate of the limiting magnitude that can be reached with respect to the background level in the image. Note that this limiting magnitude is computed with a rather simple, all-purpose algorithm, and is meant only as an approximate indication; it should not be used for any detailed calculations. Image statistics are given separately for each CCD.

The second part of the package presents the data exposure by exposure. Usually there are three pages for each exposure: the first two pages are grayscale representations of the image (one containing all four chips together, the other featuring the PC only), and the third summarizes various exposure characteristics, flags and error conditions that might arise. The grayscale presentation on the first page of the four chips together is a crude mosaic; each chip is rotated and placed in the correct position with respect to the others, but the overlap and the small differential rotations between chips (see Chapter 24) are not corrected for. The next page presents the PC by itself, at a larger scale that brings out smaller details not evident in the mosaic. This third page, giving dataset information, is divided into several zones, each summarizing information on a specific topic: the HST Spacecraft Performance Summary, with information on pointing and jitter; the Pipeline Processing Summary, with information on whether the file was processed properly by the pipeline (see Chapter 26); the Calibration Data Quality Summary, where any inconsistencies in the choices of calibration files are highlighted; the Exposure Summary, which details when and how the exposure was taken, and the Calibration Status Summary, which reports all reference files used in the calibration and their pedigree, if available. Some basic consistency checks are carried out, and the user is alerted to any potential problems thus discovered.

A few notes are in order regarding the grayscale representation of the data. The images are presented as they appear after the standard pipeline processing (see Chapter 26). Bias, standard dark, and flatfield corrections have been applied, but hot pixels and cosmic rays are not removed; hence the mottled appearance of many images, especially those with exposure times longer than a few hundred seconds. In order to limit the size of the printouts, images are block-averaged ( $2 \times 2$ ) before printing, causing some details to be lost. In general, because of the limited resolution of even good black-and-white printers, finer image details are lost; the grayscale images cannot in any way replace even a quick look on the screen.

Paper products shipped before August 1997 differ in two main respects. First, they do not have the visit-level summary of observations; some of the information is available via the tape log, but without any data quality flags or image statistics. Second, the exposure-level information is presented in a different way: the dataset information page consists simply of a printout of the PDQ file (See “Data Files and Suffixes” on page 25-1.). The grayscale images are produced by a different task, which gives them a different appearance, but the overall information content in them is very similar. Sample paper products in the new format are shown in

Figure 25.3. Users who have received paper products in the old format can regenerate them in the new format using **pp\_dads**.

**Figure 25.3:** Paper Products: List of Targets and Observations

<b>Visit: 35</b>	<b>Proposal: 05370</b>	<b>WFPC2</b>
------------------	------------------------	--------------

*Target List*

Target Name	R.A. (J2000)	Dec. (J2000)	Description
HI-LAT	13:27:11.62	-47:29:54.8	STARS; GALAXIES;

*Observation List*

Logsheet Line#	Rootname	Target Name	Operating Mode	Serials/ Gain	Aperture or FOV	Filters	Wavelength	Exposure (sec)	Quality Flags		
									Obs	Proc	Cal
35.000	U27R8502T	HI-LAT	FULL	OFF/7.00	WFALL	F814W	8006.80	600.0	○	○	○
35.000	U27R8501T	HI-LAT	FULL	OFF/7.00	WFALL	F814W	8006.80	600.0	○	○	○
39.000	U27R9U01T	HI-LAT	FULL	OFF/7.00	WFALL	F814W	8006.80	700.0	○	○	○
39.000	U27R9U02T	HI-LAT	FULL	OFF/7.00	WFALL	F814W	8006.80	700.0	○	○	○

Quality flags:    ○ = OK    ● = Not OK    Blank = Unknown or file missing

**Figure 25.4:** Paper Products: Observation Statistics (separately for each CCD)

<b>Visit: 35</b>	<b>Proposal: 05370</b>	<b>WFPC2</b>
------------------	------------------------	--------------

*Observation Statistics*

Logsheet Line#	Rootname	Target Name	Filter	Exposure Time	POSTARG	Detector	Modal Sky	Sky Sigma	Min DN	Max DN	Limiting Mag.	
35.000	U27R8502T	HI-LAT	F814W	600.00	N/A	N/A	1	6.14	2.51	-359.14	18101.54	28.82
35.000	U27R8502T	HI-LAT	F814W	600.00	N/A	N/A	2	27.68	20.75	-1126.21	52096.83	26.74
35.000	U27R8502T	HI-LAT	F814W	600.00	N/A	N/A	3	40.38	72.99	-410.52	92238.00	25.47
35.000	U27R8502T	HI-LAT	F814W	600.00	N/A	N/A	4	56.39	90.57	-1382.49	125202.3	25.14
35.000	U27R8501T	HI-LAT	F814W	600.00	N/A	N/A	1	9.37	2.60	-300.12	35567.71	28.78
35.000	U27R8501T	HI-LAT	F814W	600.00	N/A	N/A	2	66.88	20.56	-1131.11	287711.6	26.75
35.000	U27R8501T	HI-LAT	F814W	600.00	N/A	N/A	3	43.30	68.34	-576.75	108361.5	25.54
35.000	U27R8501T	HI-LAT	F814W	600.00	N/A	N/A	4	55.46	89.38	-1570.77	124874.8	25.15
39.000	U27R9U01T	HI-LAT	F814W	700.00	N/A	N/A	1	20.07	4.14	-302.07	103304.2	28.45
39.000	U27R9U01T	HI-LAT	F814W	700.00	N/A	N/A	2	38.79	30.39	-1315.45	110014.1	26.49
39.000	U27R9U01T	HI-LAT	F814W	700.00	N/A	N/A	3	43.25	90.29	-649.44	76723.60	25.41
39.000	U27R9U01T	HI-LAT	F814W	700.00	N/A	N/A	4	60.14	103.00	-1845.88	123228.6	25.16
39.000	U27R9U02T	HI-LAT	F814W	700.00	N/A	N/A	1	6.01	2.70	-354.96	12388.22	28.91
39.000	U27R9U02T	HI-LAT	F814W	700.00	N/A	N/A	2	42.91	25.78	-1234.59	121265.8	26.67
39.000	U27R9U02T	HI-LAT	F814W	700.00	N/A	N/A	3	71.66	88.56	-815.84	266563.8	25.43
39.000	U27R9U02T	HI-LAT	F814W	700.00	N/A	N/A	4	66.55	104.06	-1770.08	157240.0	25.15

Figure 25.5: Paper Products: Combined Grayscale Display

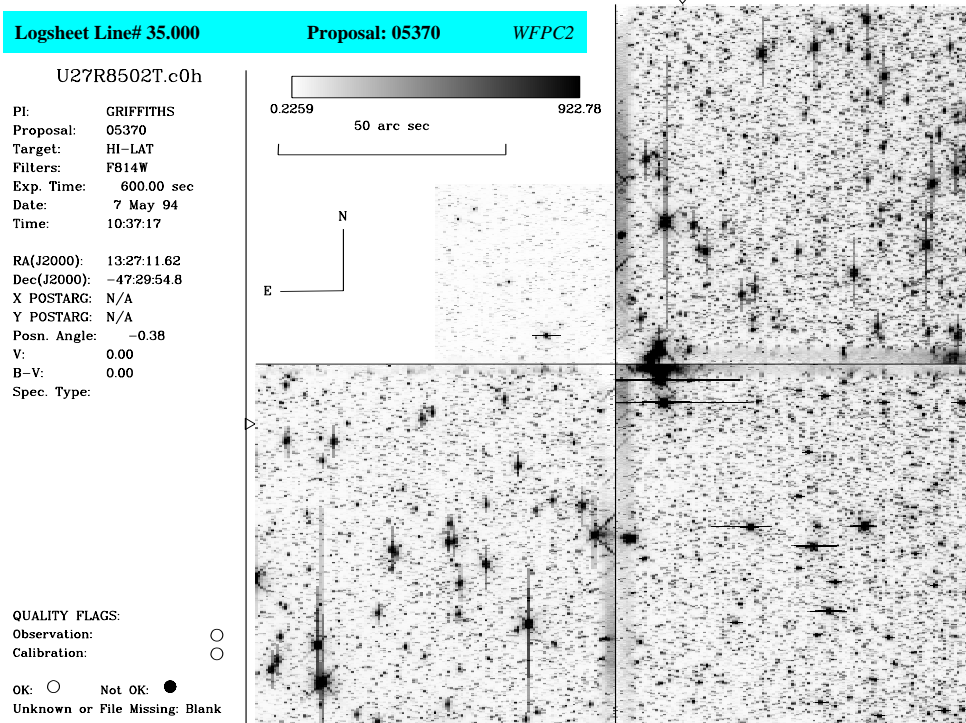


Figure 25.6: Paper Products: Observation Summary

Logsheet Line# 35.000	Observation: U27R8502T	Proposal: 05370	WFPC2
<p><i>HST Spacecraft Performance Summary</i></p> <p># Recenterings: # Losses of Locks:                      V2 Jitter (RMS): V2 Jitter (PP):                      V3 Jitter (RMS): V3 Jitter (PP):</p> <p>Could not find JITTER file.                      Very highly packed star field.                      Brighter stars saturated and blooming. Filter F814W, exposure 600s</p>		<p><i>Exposure Summary</i></p> <p>Target Name: HI-LAT                      RA (J2000): 13:27:11.62                      Dec (J2000): -47:29:54.8                      X POSTARG: N/A                      Y POSTARG: N/A                      Aperture: WFALL                      Exp Time (sec): 600.0</p>	
<p><i>Pipeline Processing Summary</i></p> <p>No Error Checks Made.</p>		<p>Rootname: U27R8502T                      Date: 7 May 94                      Time: 10:37:17                      Proposal: 05370                      PI: GRIFFITHS</p>	
<p><i>Calibration Data Quality Summary</i></p> <p>No Anomalies.</p> <p>No Calibration File Pedigree Information available.</p>		<p>Chip 3 Statistics</p> <p>Sky: 40.38                      Sky Sigma: 72.99                      Minimum: -410.52                      Maximum: 92238.00                      Limiting Mag: 25.47</p>	

Calibration Status Summary

Switches and Flags		Reference Files and Tables			
Keyword	Value	Calibration Step	Keyword	filename	Pedigree
MASKCORR	COMPLETE	Mask Correction	MASKFILE	uref\$e2112084u.r0h	
ATODCORR	COMPLETE	A-to-D Correction	ATODFILE	uref\$dbu1405iu.r1h	
BLEVCORR	COMPLETE	Bias Level Correction	BLEVFILE	ucal\$u27r8502t.x0h	
BLASCORR	COMPLETE	Bias Correction	BLASFILE	uref\$e4p1629bu.r2h	
DARKCORR	COMPLETE	Dark Correction	DARKFILE	uref\$e1q1433du.r3h	
FLATCORR	COMPLETE	Flat Field Correction	FLATFILE	uref\$e391434fu.r4h	
SHADCORR	OMIT	Shaded Shutter Correction	SHADFILE	uref\$e371355eu.r5h	
DOPHOTOM	COMPLETE	Populate Photometry Keywords	PHOTTAB	ucal:u27r8502t.c3t	



# WFPC2 Calibration

### In This Chapter...

Overview of Pipeline Calibration / 26-3

Standard Pipeline Calibration / 26-5

Recalibration / 26-10

Post-Pipeline Calibration / 26-15

This chapter discusses the *calibration* of WFPC2 data, namely the routine processing that is required before detailed data analysis is performed. We begin by describing the pipeline calibration that occurs before the data are delivered to the original observer and stored in the Hubble Data Archive. We then detail possible reasons to repeat this routine calibration and the options available to do so. Finally, we mention a few additional steps that can be taken to enhance and complement the routine pipeline processing.

After WFPC2 observations have executed, the image data pass through the OPUS *pipeline*, where they are processed and calibrated. All of the steps performed by the pipeline are recorded in the trailer file for each dataset. Figure 26.1 shows an example of a trailer file and identifies comments made during the following pipeline steps:

1. The data are partitioned (separated into individual files, e.g., the engineering and science data are separated).
2. The data are edited to insert fill (an arbitrary assigned value given in the header) in place of missing data.
3. The data are evaluated to determine discrepancies between the subset of the planned and executed observational parameters.
4. The data are converted to a generic format and the header keywords populated.
5. The data are calibrated using a standard WFPC2-specific calibration algorithm and the best available calibration files.

Figure 26.1: Sample Trailer File

```

CECCCM-***** OBSERVER COMMENTS FILE *****
CECCBN-*****
OSS quality/utility report - Wide Field/Planetary Camera II (WFII)

Observation: Object name: Proposal ID: Executed (UT):
U28S0303 PSR1957+20 05390 94.242/ 21:57:17

Observation Specifics
-----
Science Data Mode: IMAGE
CCDs Used: ALL
Data Format: STDMODE
Pointing Control: FINELOK
Filter(s): F675W
Analog gain: 7.5 electrons/DN
Exp. time (sec): 600

Comments: This observation appears to have executed as planned.

OSS staff did not inspect the observation.

No terminator crossings occurred during this observation.

OSS_INFO1: OK - no apparent problems
OSS_INFO2: NO-MON - obs not monitored (lack of eng data and/or OSS staffing)
DPPBAN-***** TRAILER FILE *****
DPPSTA----- DATA PARTITIONING STARTED -----
DPPSTR-DATA PARTITIONING STARTED: 31-AUG-94 16:15:55 .
DPPOBS-Observation Identification: Program Number 28S , Observation Set Number 03 , Observation Number 03
DPPCAT-Msg Artifacts Catalog: DCF Msg 7 contained data for Info Set File with Root Name of U28S0303P
DPPRST-Missing pkts processing is complete, processed 3200 science pkts, detected 0 as missing
DPVWM1-Weighted Quality Measure of 0 was calc for errors reported in Quality & Acctg Capsule entries for Info Set
DPPNPR- 3201 packets expected, 3201 packets received ( 1 SHPs, 0 UDLs, 0 Bad pkts) for Info Set U28S0303P
DPPEND-DATA PARTITIONING ENDED: 31-AUG-94 16:23:06 .
DPPFIN----- DATA PARTITIONING COMPLETED -----
CPEOST----- DATA EDITING STARTED -----
CPESTR-DATA EDITING STARTED 31-AUG-94 16:23:20 FOR U28S0303P.
DPE4PC- 0 fill source packets were inserted by PODPS.
DPE4DC-In U28S0303P, 0 source packets were found that contain fill data inserted by the ST DCF.
DPERSC-CP34SE: ...and 0 packets were found to have segments without Reed Solomon corrections
CPEEND-DATA EDITING ENDED 31-AUG-94 16:23:20 FOR U28S0303P.
CPEOEN----- DATA EDITING COMPLETED -----
CPGOVS----- DATA EVALUATION STARTED -----
DPVSTR-DATA EVALUATION STARTED 31-AUG-94 16:23:39 FOR U28S0303P.
DPVEND-DATA EVALUATION ENDED 31-AUG-94 16:24:03 FOR U28S0303P.
DPVWM2-Weighted Quality Measure of 0 was calc for discrepancies between predicted & actual Flags & Indicators for Info S
DPVOKK-Info Set quality was OK as Weighted Quality Measure of 0 did not exceed Quality Threshold of 9
CPGOVE----- DATA EVALUATION COMPLETED -----
CGAI00-----
CGAI01-----WIDE FIELD AND PLANETARY CAMERA GENERIC CONVERSION BEGINNING-----
CGAI00-----
CGAT01-Routine CGWFP2, version 34.4.A , will perform generic conversion
CGAT02-GENERIC CONVERSION BEGINNING: processing information set U28S0303P
CGAT03-CGWFP2 START: 31-AUG-94, 16:24:04
CGAW06-No error values detected in flags and indicators
CGAI06-SHP generic conversion has completed successfully
CGAC02-Generated new WFII reference file catalog : CCC:[SIS.WF2]U28S0303P.CTX
CGAI08-SCI generic conversion has completed successfully
CGAI22-DQM generic conversion has completed successfully
CGAT04-GENERIC CONVERSION TERMINATING: successful completion
CGAT09-CGWFP2 END: 31-AUG-94, 16:27:45
CPGOEN----- GENERIC CONVERSION COMPLETED -----
CCAI00-----
CCAI07-CALIBRATION BEGINNING: processing information set 31-AUG-94
CCAI00-----
CCAI07-CALIBRATION BEGINNING: processing information set U28S0303P
CCAI11-CWFP2 START: 31-AUG-94, 16:33:17
CCAIRI --- WF/PC-2 Calibration Starting: CALWP2 Version 1.3.0.6
CCAIRI --- Starting CALWP2: Input = U28S0303P Output = ucal:u28s0303p
CCAIRI --- Starting processing of element 1
CCAIRI photmode = WFPC2,1,A2D7,F675W,,CAL
CCAIRI --- Starting processing of element 2
CCAIRI photmode = WFPC2,2,A2D7,F675W,,CAL
CCAIRI --- Starting processing of element 3
CCAIRI photmode = WFPC2,3,A2D7,F675W,,CAL
CCAIRI --- Starting processing of element 4
CCAIRI photmode = WFPC2,4,A2D7,F675W,,CAL
CCAIRI --- Computing image statistics of element 1
CCAIRI --- Computing image statistics of element 2
CCAIRI --- Computing image statistics of element 3
CCAIRI --- Computing image statistics of element 4
CCAIRI --- WF/PC-2 Calibration Ending for observation
CCAI10-CALIBRATION END: 31-AUG-94, 16:38:30

```

1 Partitioning

2 Editing

3 Evaluation

4 Conversion

5 Calibration

The calibration software used by the pipeline is the same as that provided within STSDAS (**calwp2**). The calibration files and tables used are taken from the Calibration Data Base (CDBS) at STScI and are the most up-to-date calibration files available at the time of processing. All CDBS files are available to you through the HST Data Archive. (See Chapter 1).

## 26.1 Overview of Pipeline Calibration

In this section we provide an overview of the steps comprising the routine pipeline calibration. The flow of the data through the pipeline is presented in schematic form in Figure 26.2. The pipeline calibration software (which the user can find as **calwp2** in the STSDAS **hst\_calib** package) takes as input the raw WFPC2 data file pairs (see Table 25.1) `.d0h/.d0d`, `.q0h/.q0d`, `.x0h/.x0d`, `.q1h/.q1d` and any necessary calibration reference images or tables. The software determines which calibration steps to perform by looking at the values of the calibration switches (e.g., MASKCORR, BIASCORR, etc.) in the header of the raw data (`.d0h`) file. Likewise, it selects the reference files to use in the calibration of your data by examining the reference file keywords (e.g., MASKFILE, BIASFILE, BIASDFILE, etc.). The appropriate values of the calibration switches and reference file keywords depend on the instrumental configuration used, the date of the observation, and any special pre-specified constraints. They were initially set in the headers of the raw data file in the OPUS pipeline during generic conversion; if reprocessing is necessary, they can be redefined by editing the raw header (`.d0h`) using the task **chcalpar** and then running **calwp2** on the raw files.

The values of the calibration switches in the headers of the raw and calibrated data indicate what calibration steps the pipeline applied to the data and which calibration reference files were used. Calibration switches will have the value PERFORM, OMIT, or COMPLETE, depending on whether the step has yet to be performed, is not performed during the processing of this dataset, or was completed. For convenience, these keywords are reported in the dataset information page of the new-style paper products.

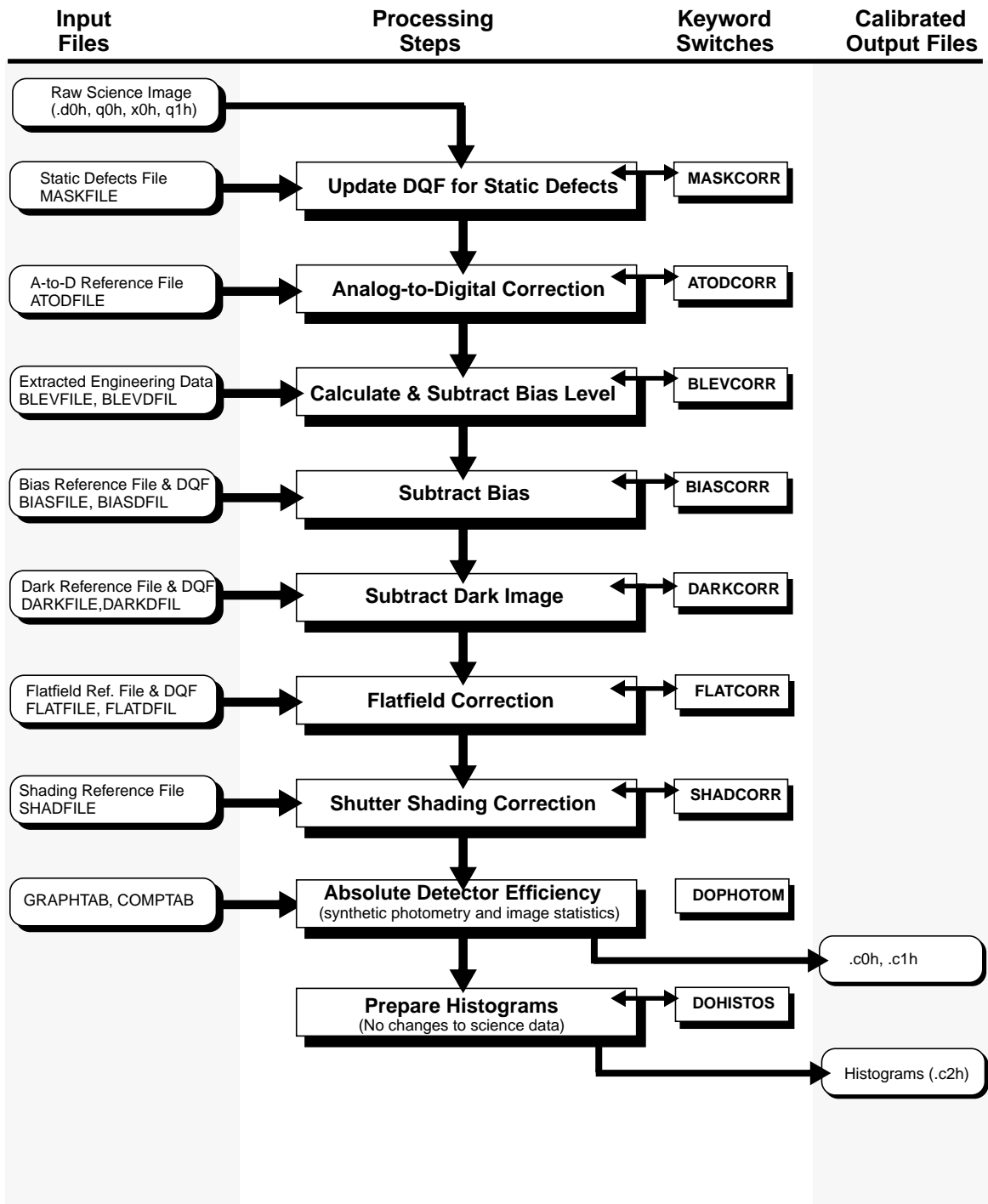
As with other header keywords, the calibration keywords can be viewed using, for example, **imhead** or **hedit**. Alternately, you can use the **chcalpar** task in the STSDAS **tools** package to view the calibration keywords directly.



There are history records at the bottom of the header file of the calibrated data (as well as the calibration reference file headers). These history records sometimes contain important information regarding the reference files used to calibrate the data in the pipeline.

The flow chart below summarizes the sequence of calibration steps performed by **calwp2**, including the input calibration reference files and tables, and the output data files from each step. The purpose of each calibration step is briefly described in the accompanying table; a more detailed explanation is provided in the following section.

Figure 26.2: Pipeline Processing by calwp2



WFPC2 / 26

**Table 26.1:** Calibration Steps and Reference Files Used for WFPC2 Pipeline Processing

Switch	Processing Step	Reference File
MASKCORR	Update the data quality file using the static bad pixel mask reference file (maskfile), which flags defects in the CCD that degrade pixel performance and that are stable over time.	maskfile (r0h)
ATODCORR	Correct the value of each pixel for the analog-to-digital conversion error using information in the A/D lookup reference file (atodfile).	atodfile (r1h)
BLEVCORR	Subtract the mean bias level from each pixel in the science data. Mean values are determined separately for even column pixels (group parameter BIASEVEN) and odd column pixels (BIASODD) because the bias level exhibits a column-wise pattern that changes over time.	blevfile, blevdfil (x0h/ q1h)
BIASCORR	Subtract bias image reference file (biasfile) from the input science image and update output data quality file with bias image data quality (biasdfil).	biasfile, biasdfil (r2h/b2h)
DARKCORR	Correct for dark current by scaling dark image reference file and subtracting it from science data. Dark image is multiplied by total dark accumulation time (keyword DARKTIME).	darkfile, darkdfil (r3h/b3h)
FLATCORR	Correct for pixel-to-pixel gain variation by multiplying by flatfield image.	flatfile, flatdfil (r4h/b4h)
SHADCORR	Remove shading due to finite shutter velocity (exposures less than 10 seconds)	shadfile (r5h)
DOPHOTOM	Determine absolute sensitivity using throughputs in <b>synphot</b> tables identified in GRAPHTAB and COMPTAB. This step does not change science data values.	
DOHISTOS	Create 3-row image (.c2h) for each group. Row 1 is a histogram of raw science values, row 2 the A/D correction, row 3 the calibrated image. (Optional, default is not to produce them.)	

## 26.2 Standard Pipeline Calibration

Each calibration step (and the keyword switches used to turn the step on or off) is described in detail in the following sections; the steps are performed in the following order:

1. Flag static bad pixels.
2. Do analog-to-digital (A/D) correction.
3. Subtract bias level.

4. Subtract bias image.
5. Subtract dark for exposures longer than 10 seconds.
6. Multiply by flatfield.
7. Apply shutter shading correction to exposures of less than 10 seconds.
8. Calculate photometry keywords.
9. Calculate histograms.
10. Generate final science data quality file.

### 26.2.1 Calibration Files

Table 26.2 lists the types (and related suffixes) of the WFPC2 reference files used in the pipeline calibration. Most suffixes have the form  $rN_h/rN_d$ , where  $N$  is a number that identifies the step in which the file is used. The related data quality file, if it exists, has the suffix  $bN_h/bN_d$ . The rootname of a reference file is based on the time that the file was delivered to the Calibration Data Base System (CDBS). The file names and history of all WFPC2 reference files in CDBS (and retrievable from the HST Archive) are contained in the Reference File Memo, available via the WFPC2 WWW pages. This memo is routinely updated with each new delivery. Any CDBS file is available for retrieval through the HST Data Archive (see Chapter 1). Some additional reference files generated by the WFPC2 IDT are listed in the IDT Reference File Memo, also available on the web. The WFPC2 web page can be found at:

[http://www.stsci.edu/ftp/instrument\\_news/WFPC2/Wfpc2\\_top.html](http://www.stsci.edu/ftp/instrument_news/WFPC2/Wfpc2_top.html)

**Table 26.2:** WFPC2 Calibration Reference Files

Suffix	Reference File
$r0_h, r0_d$	Static mask
$r1_h, r1_d$	Analog-to-digital look-up table
$r2_h, r2_d, b2_h, b2_d$	Bias
$r3_h, r3_d, b3_h, b3_d$	Dark frame
$r4_h, r4_d, b4_h, b4_d$	Flatfield
$r5_h, r5_d$	Shutter shading
$c3_f$	Photometry table (generated, not required)

All of the installed reference files contain HISTORY keywords at the end of the header which can be viewed using the **imhead** task. These keywords contain more detailed information about how the file was created and installed in the database.

## 26.2.2 Calibration Steps

### Application of the Static Mask

The static mask reference file (.r0h/.r0d) contains a map of the known bad pixels and columns. If this correction is performed (MASKCORR=PERFORM), the mask is included in the calibration output data quality files. The mask reference file is identified in the MASKFILE keyword. The science data themselves are *not* changed in any way; the STSDAS task **wfixup** can be used on the final calibrated science image (.c0h/.c0d) to interpolate across bad pixels flagged in the final data quality file (.c1h).

### A/D Correction

The analog-to-digital (A/D) converter takes the observed charge in each pixel in the CCD and converts it to a digital number. Two settings, or gains, of the A/D are used on WFPC2. The first converts a charge of approximately seven electrons to a single count (called a *Data Number* or *DN*), and the second converts a charge of approximately 14 electrons to a DN, also referred to as *gain 15* for historical reasons. A/D converters work by comparing the observed charge with a reference and act mathematically as a “floor” function. However, these devices are not perfect, and some values are reported more (or less) frequently than they would be by a perfect device. One can adjust statistically for this bias; fortunately the WFPC2 A/D converters are relatively well-behaved and this is a small correction. The largest correction is about 1.8 to 2.0 DN for bit 12 (thus 2048).

The best estimate of the A/D bias is removed when the ATODCORR keyword is set to PERFORM. The calibration file used to correct for the A/D errors has the suffix .r1h.

### Bias Level Removal

The charges that are in each pixel sit on top of an electronic pedestal, or “bias” designed to keep the A/D levels consistently above zero. The mean level of the bias must be determined empirically using extended register (overscan) pixels which do not view the sky. The values of these pixels are placed in the extracted engineering files (.x0h/.x0d). The overscan area used to calculate the mean bias levels is [9:14,10:790], with BIASODD being determined from columns 10, 12, and 14 and a BIASEVEN being determined from columns 9, 11, and 13 (this surprising nomenclature is due to an offset in the .x0h file; even and odd are correctly oriented with respect to the data file columns). In observations before March 8, 1994, the pipeline used a larger part of the overscan region, resulting in oversubtraction of the bias level and possibly large negative pixel values. Separate even and odd bias levels were extracted only after May 4, 1994. See Chapter 27 for more information on how to deal with early WFPC2 data. The keyword BLEVCORR controls the subtraction of the bias in **calwp2**.

### Bias Image Subtraction

The value of the bias pedestal can vary with position across the chip. Therefore, once the mean bias level correction has been completed, the pipeline looks at the keyword BIASCORR. If it is set to PERFORM, then a bias image (.r2h) is subtracted from the data to remove any position-dependent bias pattern. The bias reference file is generated from a large set of A/D and bias-level

corrected zero-length exposures. The correction consists of subtracting the bias file from the observation and flagging in the `.c1h/.c1d` file any bad pixels noted in the bias data quality file (`.b2h/.b2d`).

### Dark Image Subtraction

A dark correction is required to account for the thermally-induced dark current as well as a *glow* (see “Dark Glow” on page 27-4) from the field flattening lens. The dark reference file is generated from ten or more individual dark frames (long exposures taken with the shutter closed) that have each had the standard calibration corrections applied (ATODCORR, BLEVCORR, and BIASCORR). In addition, each frame is examined and regions affected by image anomalies (such as residual images, see Figure 27.2) are masked out. If a dark correction is performed, the dark reference file (which was normalized to one second) is scaled by the DARKTIME keyword value and subtracted from the observation. The keyword DARKCORR controls the subtraction of the dark file (`.r3h`). By default, DARKCORR is set to “PERFORM” for all exposures longer than 10 seconds, and to “OMIT” for shorter exposures.

### Flatfield Multiplication

The number of electrons generated in a given pixel by a star of a given magnitude depends on the individual quantum efficiency of the pixel as well as any large scale vignetting of the field-of-view caused by the telescope and camera optics. To correct these variations in total quantum efficiency, the image is multiplied by an inverse flatfield file, which is currently generated from a combination of on-orbit data, used to determine the large-scale structure of the illumination pattern, and data taken before launch to determine the pixel-to-pixel response function. The application of the flatfield file (extension `.r4h`) is controlled by the keyword FLATCORR.

### Shutter Shading Correction

The finite velocity of the shutter produces a position-dependent exposure time. This effect is only significant for exposures of a few seconds or less, and is automatically removed from all exposures less than ten seconds. The keyword switch is SHADCORR, and the shutter shading file name is stored in the keyword SHADFILE.

### Creation of Photometry Keywords

Photometry keywords, which provide the conversion from calibrated counts to astronomical magnitude, are created using the STSDAS package **synphot**. (More information on **synphot** can be found in this document, and in the *Synphot User's Guide*, which is available via WWW.) These keywords are listed in Figure 26.3, below; the first two keywords are in the ASCII header (both `.d0h` and `.c0h`) while the last five keywords are group parameters (use the IRAF tasks **imheader** or **hedit** to examine the group keywords—see Chapters 2 and 3 for more details). This calibration step uses the HST graph and component tables (`.tmg` and `.tmc`) to determine the throughput for the appropriate WFPC2 observing mode and filter. The keyword switch for this step is DOPHOTOM, and the reference file keywords are GRAPHTAB and COMPTAB.

**Figure 26.3: Photometry Keywords**

<b>Header parameters</b>	DOPHOTOM= 'YES ' / Fill photometry keywords: YES, NO, DONE
	PHOTTAB = 'ucal\$u27s0301n.c3t' / name of the photometry calibration table
	'PHOTMODE' / Photometry mode (for example, WFPC2,1, A2D7, F675W,CAL)
<b>Group parameters</b>	'PHOTFLAM' / Inverse Sensitivity (erg/sec/cm <sup>2</sup> /Å for 1 DN/sec)
	'PHOTPLAM' / Pivot wavelength (angstroms)
	'PHOTBW ' / RMS bandwidth of the filter (angstroms)
	'PHOTZPT' / Photometric zeropoint (magnitude)

## Histogram Creation

Histograms of the raw data, the A/D corrected data, and the final calibrated output data are created and stored in the .c2h/.c2d image. This is a multigroup image with one group for each group in the calibrated data file. Each group contains a three-line image where the first row is a histogram of the raw data values, row two is a histogram of the A/D corrected data, and row three is a histogram of the final calibrated science data. This operation is controlled by the keyword DOHISTOS; the default is not to produce them.

## Data Quality File Creation

The **calwp2** software will combine the raw data quality file (.q0h, .q1h) with the static pixel mask (.r0h) and the data quality files for bias, dark, and flatfield reference files (.b2h, .b3h, .b4h) in order to generate the calibrated science data quality file (.c1h). The flag values used are defined below. The final calibrated data quality file (.c1h) may be examined (for example, using SAOimage, ximtool, or **imexamine**) to identify which pixels in your science image may be bad.



The bad pixels flagged in the .c1h file have not been fixed in the .c0h file. You may wish to use the STSDAS task **wfixup** to interpolate across bad pixels in your science image or to use the .c1h file to determine which pixels to discard in various analysis programs.

## The Image

After the completion of the standard pipeline processing the final image is placed in a real-valued image labelled .c0h/.c0d.

**Table 26.3:** WFPC2 Data Quality Flag Values

Flag Value	Description
0	Good pixel
1	Reed-Solomon decoding error. This pixel is part of a packet of data in which one or more pixels may have been corrupted during transmission.
2	Calibration file defect—set if pixel flagged in any calibration file. Includes charge transfer traps identified in static pixel mask file (.r0h).
4	Permanent camera defect. Static defects are maintained in the CDBS database and flag problems such as blocked columns and dead pixels. (Not currently used.)
8	A/D converter saturation. The actual signal is unrecoverable but known to exceed the A/D full-scale signal (4095). <sup>a</sup>
16	Missing data. The pixel was lost during readout or transmission. (Not currently used.)
32	Bad pixel that does not fall into above categories.
128	Permanent charge trap. (Not currently used.)
256	Questionable pixel. A pixel lying above a charge trap which may be affected by the trap.
512	Unrepaired warm pixel.
1024	Repaired warm pixel.

a. Calibrated saturated pixels may have values significantly lower than 4095 due to bias subtraction and flatfielding. In general, data values above 3500 DN are likely saturated.

## 26.3 Recalibration

In this section we discuss the *recalibration* of WFPC2 data, namely running the raw data again through the same pipeline calibration described thus far. We will first indicate when recalibration can be advisable, usually due to the availability of improved reference files and tables, and then go through the mechanics of how recalibration is performed. The next section will discuss some relevant post-pipeline calibration issues.

### 26.3.1 Why and When to Recalibrate

The main reason to recalibrate WFPC2 images is the availability of better or more up-to-date reference files and tables, especially darks, flatfields, and **synphot** component tables, and changes in the pipeline calibration task **calwp2**. The most recent reference files and tables appropriate to a given observation can

be determined and retrieved via StarView. Note that, when recalibrating, **calwp2** must be run again in its entirety even if only one reference component has changed, and thus all reference elements need to be retrieved (see below).

In the following we give a brief summary of some relevant changes of reference elements and the pipeline task as of today. More details and up-to-date information can be found in the WFPC2 History Memo, and especially its section 5 for calibration details. We also give a quantitative account of the differences between various generations of reference files in Chapter 27. The WFPC2 History Memo is available at the following URL:

[http://www.stsci.edu/ftp/instrument\\_news/WFPC2/Wfpc2\\_memos/wfpc2\\_history.html](http://www.stsci.edu/ftp/instrument_news/WFPC2/Wfpc2_memos/wfpc2_history.html)

### Darks

The calibrated data originally delivered to the PI and to the Archive run through the pipeline calibration within a few days of the observation. At that time, the available dark reference file does not contain the most up-to-date information about warm pixels, which change on a weekly timescale (see “Warm Pixels” on page 26-16). Thus, dark files used in standard processing are *always* out of date, and the correction of warm pixels can be improved by recalibrating with a more appropriate dark file. However, another method to correct for warm pixels, the STSDAS task **warmpix** (described in “Warm Pixels” on page 26-16) can be used instead of recalibrating. Using **warmpix** is generally recommended because it gives the user more flexibility and control over the treatment of warm pixels.

Very deep observations taken before August 1996 can also benefit from recalibration with a different dark reference file. Until that date, dark reference files were produced by combining ten dark exposures taken during a two week interval surrounding the observation. For observations longer than about 20,000 s (10,000 s in the UV and in narrow-band filters), the noise in this dark frame is a significant contributor to the total noise in the final calibrated image. For this reason, if the science results are limited by the noise, it is advisable to recalibrate the image using a “superdark” reference file. Superdarks are generated from 120 individual dark exposures, compared to the ten exposures that go into a normal dark, and thus reduce significantly the noise associated with dark subtraction. If a superdark is used, the accompanying superbias must also be used, and warm pixels must be corrected independently by post-pipeline processing tasks such as **warmpix** (see “Warm Pixels” on page 26-16).

Starting August 1, 1996, the dark reference files have been generated using the appropriate superdark and adding the information on warm pixels from that week’s darks; thus, observations taken after that date do not require recalibration in order to use a superdark. (Recalibration may still be appropriate in order to use the dark reference file with up-to-date information on warm pixels.)

A description of available superdarks and how to retrieve them via the Archive can be found in sections 2 and 5 of the WFPC2 History Memo on the WFPC2 Web page.

## Flatfields

Very early observations, before March 9, 1994, used interim flat fields based on pre-launch data. These flat fields did not have good large-scale properties, with peak errors of about 10%, and thus WFPC2 observations before that date most likely need to be recalibrated. After that date, in-flight flatfields have been used. Their quality has steadily improved, and the flatfields currently in the pipeline are believed to be good to about 0.3% on small scales, and 1% or less on large scales. See Chapter 27 for a detailed discussion of the differences between various generations of flatfields.

If you are in doubt about the quality of the flatfielding in your observations, check the PEDIGREE and DESCRIP keywords of the flatfield file, also reported (after December 1994) in the HISTORY comments at the end of the header of the calibrated image. If PEDIGREE is GROUND, the data will need to be recalibrated. If the PEDIGREE is INFLIGHT, the flatfield was obtained from on-orbit data, and the DESCRIP keyword gives some information on its quality. INFLIGHT flatfields are of sufficient quality for most scientific goals, but for especially demanding applications and data with very high signal-to-noise ratio, it may be advisable to recalibrate with the most recent flatfields.

## Photometric Tables

The photometric component tables are used by **synphot** to determine the photometric calibration, namely the photometric header parameters PHOTFLAM and PHOTPLAM (see Chapter 28). These component tables have been updated several times, most recently on May 16, 1997, in order to contain the most up-to-date information on the throughput of WFPC2. If the photometric tables have changed, users can either recalibrate their observations or, more simply, run **synphot** directly to determine the header parameters. Users can also use the alternate methods given in “Photometric Zero Point” on page 28-2 to calibrate their observations, thus avoiding recalibration altogether.

## Pipeline Calibration Task **calwp2**

Another possible reason for recalibration is to use a more recent version of the calibration pipeline task **calwp2**. This task has seen several minor revisions, mostly to add information to processed data; the current version, as of this writing, is 1.3.5.2. Only three of the **calwp2** revisions since WFPC2 operations began actually affect the calibrated data. The first two were changes in how the bias level is computed: starting in March 8, 1994 (version 1.3.0.5), columns 3 through 8 of the overscan data were no longer used, because they could be affected by the image background; and starting in May 4, 1994 (version 1.3.0.6), separate bias levels were computed for even and odd columns, resulting in a slightly better image flatness for about 1% of all WFPC2 images (see *WFPC2 ISR 97-04*).

The third update (version 1.3.5.2, January 3, 1997) corrects a bug introduced in December 1994 (1.3.0.7) in the calibration of WFPC2 single-chip, two-chip, or three-chip observations that do not include the PC (about 1% of all archived observations). We recommend that such observations archived between December 1994 and January 1997 be recalibrated with the most recent version of **calwp2**.

### 26.3.2 Assembling the Calibration Files

In order to recalibrate a WFPC2 dataset, you need to retrieve *all* of the reference files and tables used by the calibration steps set to PERFORM. See “Identifying Calibration Reference Files” on page 1-19 for a description of how to obtain the appropriate reference files from the STScI Archive using StarView. Standard pipeline processing uses those files listed by StarView as the best reference files. We suggest copying the raw data files and the required reference files and tables to a subdirectory used for recalibration. This precaution will preserve all original files.

### 26.3.3 Setting Calibration Switches

The next step in recalibrating HST data is to set the calibration switches and reference keywords in the header of your raw data file (.d0h). These switches determine which calibration steps are performed and which reference files are used at each step in the process.

To change the calibration header keywords in a dataset, we recommend using at first use the **chcalpar** task in the STSDAS **hst\_calib.ctools** package. The **hedit** task provides more detailed control over individual keywords and is preferred by some users experienced with calibration of WFPC2.

The **chcalpar** task takes a single input parameter—the name(s) of the image files to be edited. When **chcalpar** starts, it automatically determines the instrument used to produce that image and opens one of several parameter sets (*pset*) that loads it with the current values of the header keywords. The WFPC2 pset is named `ckwwfp2`. Typing **ckwwfp2**, as a task name, at the `cl>` prompt will also edit this pset.

A detailed description of the steps involved in changing header keywords follows:

1. Start the **chcalpar** task, specifying the image(s) in which you want to change keyword values. If you specify more than one image, for example using wildcards, the task will take initial keyword values from the first image, but it will substitute only the keywords that are actually typed in. For example, you could change keywords for all WFPC2 raw science images in the current directory (with initial values from the first image), using the following command:

```
wf> chcalpar u*.d0h
```

2. When **chcalpar** starts, you will be placed in **epar**—the IRAF parameter editor, and will be able to edit the parameter set of calibration keywords. Change the values of any calibration switches, reference files or tables to the values you wish to use for recalibrating your data. Remember that **no** processing has been done on the raw datasets. Therefore, even if you wish to correct, for instance, only the flatfielding, you will need to redo the bias and dark current subtraction as well. Therefore the switches for all these steps must be set to PERFORM.

- Exit the editor by typing `:q` two times (the first `:q` to exit the pset editor; the second to exit the task). The task will ask if you wish to accept the current settings. If you type “y”, the settings are saved and you will return to the IRAF prompt. If you type “n”, you will be placed back in the editor to re-define the settings. If you type “a”, you will return to the IRAF prompt and any changes will be discarded. For additional examples of updating the calibration keywords, check the on-line help by typing `help chcalpar`.

The calibration reference file names in the header of the raw data (i.e., the `.d0h` file) are typically preceded by five characters (e.g., `uref$` for calibration images and `utab$` for calibration tables) which are pointers to the location on disk where the files are to be found by the calibration software. Before running the calibration routines, you will need to set these variables to the path where your reference files (and `.x0h/.q1h` raw data files) are located. For WFPC2 data, you would use something like the following:

```
to> set uref = "/nemesis/hstdata/caldir/"
to> set mtab = "/nemesis/hstdata/caldir/"
to> set ucal = "/nemesis/hstdata/rawdir/"
```

where `caldir` is the subdirectory for the reference files and `rawdir` is the subdirectory for the uncalibrated images.

While in VMS, to set the `uref`, for instance, one would type instead

```
to> set uref = "DISK$SHARE:[HSTDATA.CALDIR]"
```

where `HSTDATA.CALDIR` is the directory where you have stored the calibration reference files and tables.

Once you have correctly changed the values of the calibration keywords in the header of the raw data file, you are ready to recalibrate your data. The WFPC2 calibration software, **calwp2**, is run by typing the name of the task followed by the *rootname* of the observation dataset. For example, to recalibrate the dataset `u0w10e02t` and write the log of the results to the file `calwp2.log` (rather than to the screen), you would type:

```
wf> calwp2 u0w10e02t > calwp2.log
```




---

Note that the calibration routine will not overwrite an existing calibrated file. If you run the calibration tasks in the directory where your calibrated data already exist, you will need to specify a different output file name, for example:

```
wf> calwp2 u00ug201t wfpc_out > wfpc.log
```

---

For more information about how these routines work, use the on-line help by typing `help calwp2`.

### Calculating Absolute Sensitivity for WFPC2

If you set `DOPHOTOM=OMIT` before running **calwp2**, then the values of inverse sensitivity (`PHOTFLAM`), pivot wavelength (`PHOTPLAM`), RMS bandwidth (`PHOTBW`), zeropoint (`PHOTZPT`), and observation mode (`PHOTMODE`) will not be written to the header of the recalibrated data file.

Remember that the DOPHOTOM calibration step does not alter the values of the data (which are always counts or data numbers in the calibrated file), but only writes the information necessary to convert counts to flux in the header of the file. Therefore, unless you wish to recalculate the absolute sensitivity for your observation (e.g., because a more recent estimate of the throughput exists for your observing mode), there is no need to recompute these values and you can simply use the keyword values from your original calibrated file and apply them to your recalibrated data. However, new estimates of WFPC2 transmission and absolute sensitivity were obtained in September 1995, May 1996, and May 1997. If your data were processed in the pipeline before May 1997, you may wish to re-create the absolute sensitivity parameters using the latest version of **synphot**, which contains tables based on the most recent photometric calibration of WFPC2.

If you wish to recalculate the absolute sensitivity, set DOPHOTOM=YES in the .d0h file before running **calwp2**, or alternately, use the tasks in the **synphot** package of STSDAS.




---

The section titled “synphot” on page 3-16 has more information about how to use **synphot**.

---

To calculate the absolute sensitivity, **calwp2** and the **synphot** tasks use a series of component lookup and throughput tables. These tables are not part of STSDAS itself, but are part of the **synphot** dataset, which can be easily installed at your home site (see “Getting the Synphot Database” on page A-15 for information about how to do this). A more detailed discussion of photometric calibration can be found in “Photometric Corrections” on page 28-6.




---

You *must* have retrieved the **synphot** tables in order to recalculate absolute sensitivity for WFPC2 data using **calwp2** or **synphot**.

---

## 26.4 Post-Pipeline Calibration

The calibrated individual images produced by the standard pipeline processing are, in most respects, as good as our knowledge of the instrument can make them. The usefulness of post-pipeline calibration is in general limited to two areas: improving the correction of pixels with elevated dark current (warm pixels), which are known to vary with time; and removing cosmic rays by comparing multiple images of the same field.

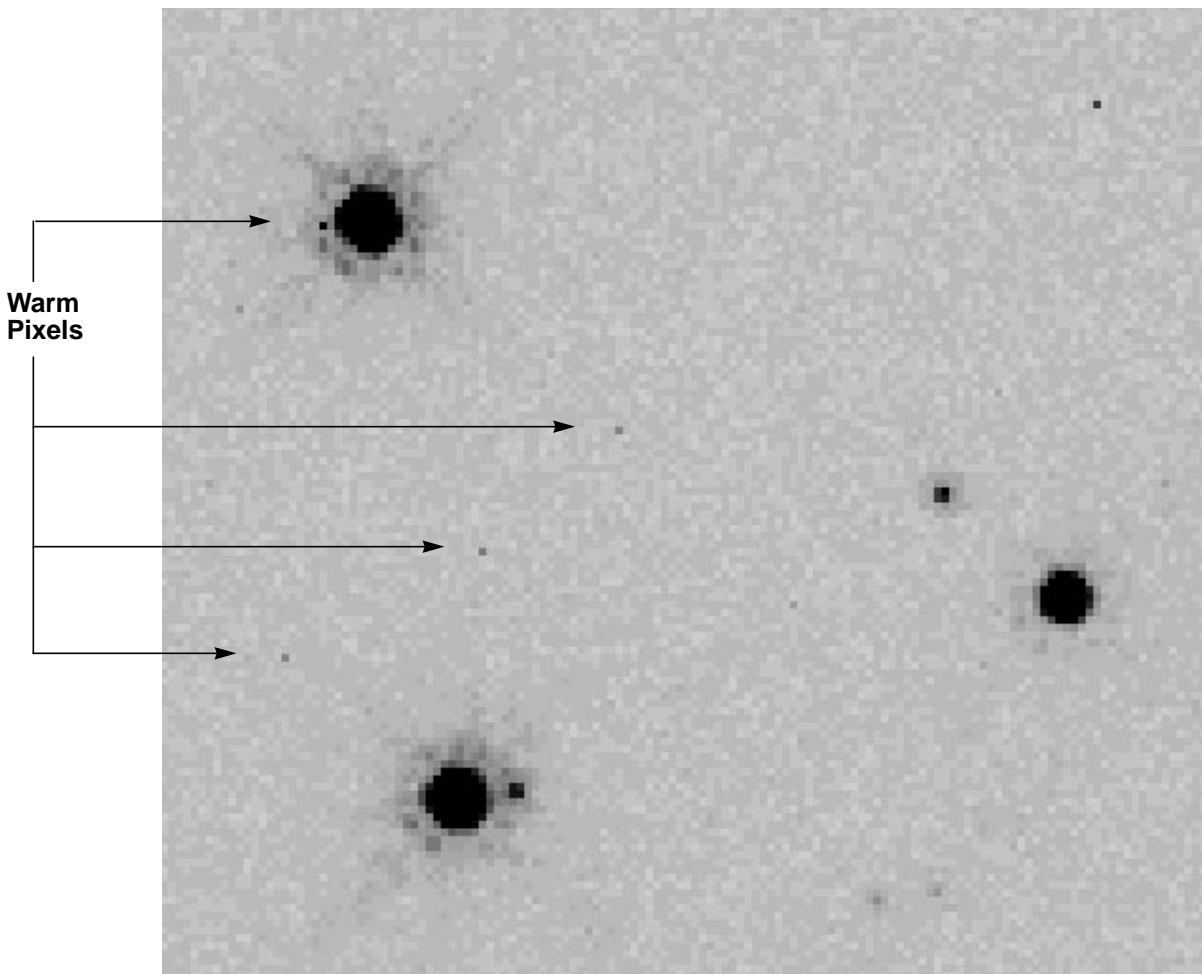


The treatment of warm pixels and cosmic rays can be quite different in the case of *dithered* data. This case is discussed in “Dithering” on page 28-19; the present discussion refers to co-aligned data only.

### 26.4.1 Warm Pixels

Figure 26.4 shows a section of a PC image of a stellar field. Cosmic rays have been removed through comparison of successive images. Nonetheless, individual bright pixels are clearly visible throughout the field.

**Figure 26.4:** PC Image of Stellar Field Showing Warm Pixels



These bright pixels are *warm* pixels, or pixels with an elevated dark current. The vast majority of WFPC2 pixels have a total dark current of about  $0.005 \text{ e}^-/\text{s}^{-1}$  (including the *dark glow*, discussed in “Dark Glow” on page 27-4). However, at

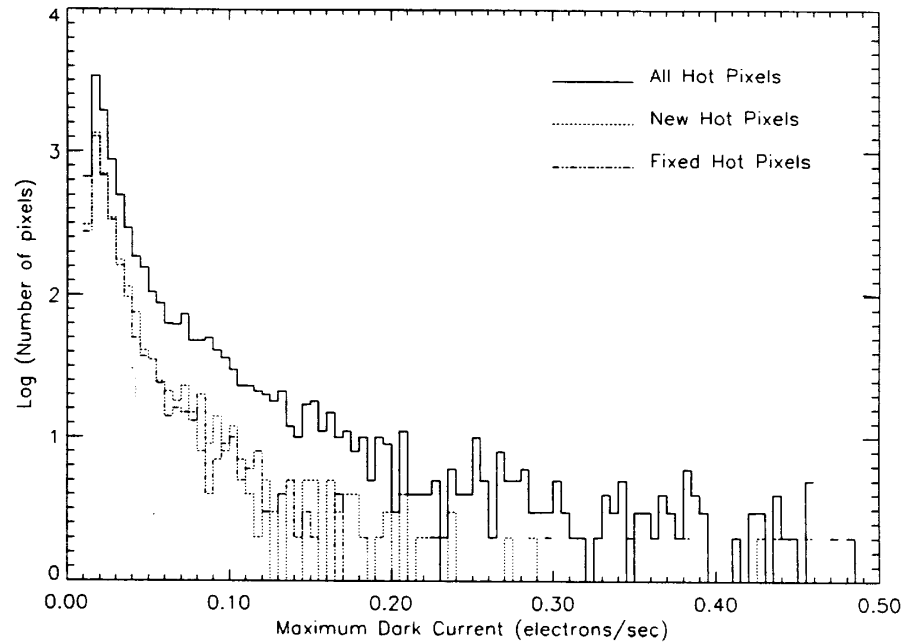
any given time there are a few thousand pixels in each CCD, called warm pixels, with a dark current more than  $0.02 \text{ e}^-/\text{s}^{-1}$ , up to several  $\text{e}^-/\text{s}^{-1}$  in a few cases (see Figure 26.5). Some of these pixels are permanently warm, but most become warm during the course of the month, probably as a consequence of the on-orbit bombardment by heavy nuclei. STIS, the other instrument currently aboard HST that uses CCDs, exhibits a similar behavior. Most warm pixels return to normal after the CCDs are brought to room temperature for a few hours.

To repair warm pixels we run monthly decontaminations, in which the instrument warms up to about 22 C for a period of six hours. (Longer decontaminations do not appear to improve the fraction of pixels fixed.) Decontaminations are also needed to let UV-blocking contaminants that build up on the CCD windows evaporate, thus temporarily restoring the UV throughput of the camera. For more detailed information, see the *WFPC2 Instrument Handbook*.

Because of the time variability of warm pixels, standard dark correction does not deal with them adequately. Even dark frames taken within a day of the observation will contain some warm pixels that vary significantly from those in the observation. We have developed a task, known as **warmpix**, that will allow a user to either flag, or attempt to correct, pixels which are known to be warm, or which have varied near the time of the observation.

### Will Warm Pixels Hurt my Science?

The impact of warm pixels on the scientific results obtained from WFPC2 images depends on a number of factors: the exposure length, the number of objects, and the science goals. If the principal goal of the program is to acquire morphological information on well-resolved targets, warm pixels are usually not a serious concern, as they are easily recognizable. If the goal is accurate photometry of point sources, the probability that uncorrected warm pixels will influence the measurement at a given level can be computed on the basis of the distribution of warm pixels (Figure 26.5). In general, warm pixels are a concern in two cases: accurate photometry of faint sources in crowded fields, where warm pixels can easily be confused with cores of faint sources, or aperture photometry with very large apertures and/or of extended objects. In the latter case, warm pixels cause a positive tail in the count distribution that is not included in the background determination, but—depending on the software used—could be included in the integrated source flux, which will then be positively biased.

**Figure 26.5:** Distribution of Dark Current for Warm Pixels

### Can Warm Pixels be Corrected?

There are two levels of possible correction for warm pixels. The first is to identify and flag the warm pixels. Depending on the software used, the flagged pixels can either be ignored (PSF fitting software generally allows this) or be interpolated from nearby pixels (for software that requires a valid value for all pixels, such as most aperture photometry tasks). The identification of warm pixels can be accomplished by taking advantage of the fact that they are the only WFPC2 feature to extend across only one pixel; both cosmic rays and photons, in the form of point sources, involve more than one pixel. The IRAF task **cosmicrays**, written originally to remove single-pixel cosmic rays in ground-based data, has been used with some success to identify warm pixels in WFPC2 data. Identification of warm pixels is also possible using information from dark frames taken before and after the observations were executed, as described below.

The second level is to attempt subtraction of the dark current that existed at the time of the observations. This has the advantage that the information that exists in the measured signal in the pixel is retained, but it requires independent timely information on the dark current. WFPC2 takes several darks every week, thus information on warm pixels is available with a time resolution of about one week. While the user can in principle retrieve and process the darks taken at the time of observation, we provide a task and a set of tables to facilitate this process. The task is called **warmpix** and is part of the standard STSDAS release; the tables, in IRAF table format, are made available via the STScI Web pages at URL:

[http://www.stsci.edu/ftp/instrument\\_news/WFPC2/wfpc2\\_warmpix.html](http://www.stsci.edu/ftp/instrument_news/WFPC2/wfpc2_warmpix.html)

In order to use **warmpix** to identify or correct WFPC2 observations for the effect of warm pixels, perform the following steps:

- Obtain the relevant warm pixel tables from the URL previously mentioned. Each table name reflects its applicability dates; for example, the table named `decon_951214_960111.tab.Z` applies to all observations between December 14, 1995 and January 11, 1996.




---

These tables are in Unix-compressed format. On some systems, the retrieved table will not have the `.Z` extension, but they still need to be renamed to add the `.Z` extension and uncompressed by the Unix task `uncompress`. Please contact the Help Desk at `help@stsci.edu` if you have a non-Unix system or if you encounter difficulties in retrieving the tables.

---

- To correct the warm pixels, retrieve the calibration files used for dark subtraction and flatfielding in the calibrated image. The filenames are in the header parameters `DARKFILE` and `FLATFILE`, respectively. Redefine the IRAF variable `uref$` to point to the directory where the dark and flatfiles are stored. This step is required for **warmpix** to undo the dark current subtraction done in the pipeline, and substitute its own. If **warmpix** cannot find these files, it will not be able to correct the dark current subtraction, and will flag all warm pixels as bad.
- Run **warmpix** to correct and/or flag warm pixels. There are a number of user-adjustable parameters to decide which pixels should be corrected and which should be flagged as uncorrectable. Please see the **warmpix** help file for more details.

At the end of this process, pixels that exceed the user-defined thresholds will be either corrected for the dark current measured in the darks, linearly interpolated to the date of the observation, or be flagged as uncorrectable. An option is available to set the uncorrectable pixels to a specified value or to set the data quality values in the associated data quality files to reflect the fact that pixels have been corrected or rejected.

This procedure will generally correct for 90% to 95% of the warm pixels found in typical user data. There are some uncertainties in the results, associated with the intrinsic variability of hot pixels and the time span between darks. We have recently started a program to obtain dark frames daily, resulting in better warm pixel information. These darks are taken as a service to users, and they are not currently part of our delivered calibration files. Users who wish to use this information can recalibrate their data (see “Recalibration” on page 26-10) using a dark made from darks taken within one or two days of their observations.




---

Non-STSDAS tasks generally ignore the data quality files, and thus may not properly use the information indicating which pixels need to be rejected. Users should propagate this information by the appropriate method, which will depend on the specifics of the task.

---

## 26.4.2 Removing Cosmic Rays from Co-aligned Images

WFPC2 images typically contain a large number of *cosmic ray* events, which are caused by the interaction of galactic cosmic rays and protons from the Earth's radiation belt with the CCD. Hits occur at an average rate of about 1.8 events  $s^{-1}$  per CCD ( $1.2 s^{-1} cm^{-2}$ ), with an overall variation in rate of 60% (peak-to-peak) depending upon geomagnetic latitude and position with respect to the South Atlantic Anomaly (see also the *WFPC2 Instrument Handbook*, v. 4.0, pages 74-79).

Unlike events seen on the ground, most WFPC2 cosmic ray events deposit a significant amount of charge in several pixels; the average number of pixels affected is 6, with a peak signal of 1500  $e^{-}$  per pixel and a few tens of  $e^{-}$  per pixel at the edges. About 3% of the pixels, or 20,000 pixels per CCD, will be affected by cosmic rays in a long exposure (1800 s). Figure 26.6 shows the impact of cosmic rays in an 800 second exposure with WFPC2. The area shown is about 1/16th of one chip (a 200 x 200 region); pixels affected by cosmic rays are shown in black and unaffected pixels are shown in white. A typical long WFPC2 exposure (2000 s) would have about 2.5 times as many pixels corrupted by cosmic rays.

Cosmic rays are noticeable even for very short exposures. The WFPC2 electronics allow activities to be started only at one-minute intervals; thus a minimum-length exposure will collect at least one minute's worth of cosmic rays, the interval between camera reset and readout, and will be affected by about a hundred cosmic rays per CCD.

As a result of the undersampling of the WFPC2 PSF by the WF and PC pixels, it is very difficult to differentiate stars from cosmic rays using a single exposure. If multiple co-aligned images are available, cosmic rays can be removed simply and reliably by comparing the flux in the same pixel in different images, assuming that any differences well above the noise are positive deviations due to cosmic rays. STSDAS tasks such as **crrej** and **gcombine** can identify and correct pixels affected by cosmic rays in such images. (The task **crrej** has been significantly improved since the previous edition of the *HST Data Handbook* and is now the recommended choice.) If the images are shifted by an integral number of pixels, they can be realigned using a task such as **imshift**. As each CCD is oriented differently on the sky, this operation will need to be done on one group at a time, using the pixel shift appropriate for each CCD in turn.

Another consequence of the undersampling of WFPC2 is that small pointing shifts will cause measurable differences even between images at the same nominal pointing. These differences are especially noticeable in PC images, where

pointing offsets of only 10 mas can cause a difference between successive images of 10% or more near the edges of stellar PSFs. We recommend that users allow for such differences by using the multiplicative noise term included in the noise model of the task used for cosmic ray rejection (`scalenoise` for **crrej** and `snoise` for **gcombine**). For typical pointing uncertainties, a multiplicative noise of 10% is adequate; note this is specified as 10 for `scalenoise`, and 0.1 for `snoise`. It is also strongly recommended that an image mask be generated for each image, to verify if there is an undue concentration of cosmic rays identified near point sources—usually an indication that the cores of point sources are mistaken for cosmic rays. Detailed explanations of **crrej** and **gcombine** can be found in the on-line help.

**Figure 26.6:** WF Exposure Showing Pixels Affected by Cosmic Rays



Because sub-pixel dithering strategies are now very common, the image combination tasks in the **drizzle** package (see “Dithering” on page 28-19) now include a script that can remove cosmic rays from images taken at multiple pointings, without repetitions.

### How many Images for Proper CR Rejection?

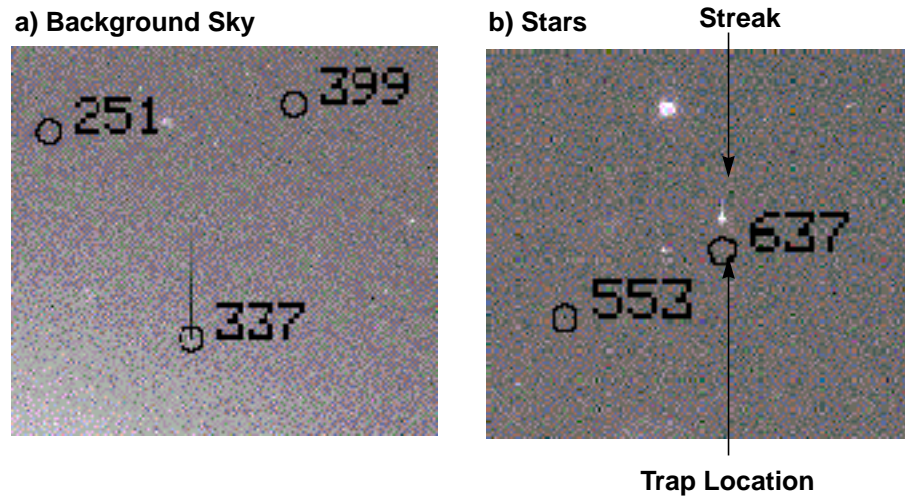
Cosmic rays are so numerous on WFPC2 images that double hits are not uncommon. For example, the combination of two 2000 s images will typically contain about 500 pixels per CCD that are affected by cosmic rays in both images; in most of these cases, the hit will be marginal in one of the two images. If the science goals require a high level of cosmic ray rejection, it will be desirable to conduct a more stringent test in pixels adjacent to detected cosmic rays (see the parameter `radius` in `crrej`). Even better would be, in the planning stage, to break the observation into more than two exposures; the WFPC2 Exposure Time Calculator gives specific recommendations on the number of exposures necessary as a function of the number of pixels lost. In general, three exposures are sufficient for non-stringent programs, and four exposures for any program. The Exposure Time Calculator is available via the WWW at:

[http://www.stsci.edu/ftp/instrument\\_news/WFPC2/Wfpc2\\_etc/wfpc2-etc.html](http://www.stsci.edu/ftp/instrument_news/WFPC2/Wfpc2_etc/wfpc2-etc.html)

### 26.4.3 Charge Traps

There are about 30 pixels in WFPC2 which do not transfer charge efficiently during readout, producing artifacts that are often quite noticeable. Typically, charge is delayed into successive pixels, producing a streak above the defective pixel. In the worst cases, the entire column above the pixel can be rendered useless. On blank sky, these traps will tend to produce a *dark* streak. However, when a bright object, or cosmic ray, is read through them, a bright streak will follow the object. Figure 26.7 shows examples of both of these effects. (Note that these “macroscopic” charge traps are different from the much smaller traps believed to be responsible for the charge transfer effect discussed under “Charge Transfer Efficiency” on page 28-11.)

The images in Figure 26.7 show streaks (a) in the background sky and, (b) stellar images produced by charge traps in the WFPC2. Individual traps have been cataloged and their identifying numbers are shown.

**Figure 26.7:** Streaks in a) Background Sky, and b) Stars

Bright tails have been measured on images taken both before and after the April 23, 1994 cool down. The behavior of the traps has been quite constant with time, and fortunately there is no evidence for the formation of new traps since the ground system testing in May 1993. The charge delay in each of the traps is well characterized by a simple exponential decay which varies in strength and spatial scale from trap to trap.

The positions of the traps, as well as those of pixels immediately above the traps, are marked in the .c1h data quality files with the value of 2, indicating a chip defect. These pixels will be obviously defective even in images of sources of uniform surface brightness. However, after August 1995 the entire column above traps has been flagged with the value of 256, which indicates a “Questionable Pixel.” An object with sharp features (such as a star) will leave a trail should it fall on any of these pixels.

In cases where a bright streak is produced by a cosmic ray, standard cosmic ray removal techniques will typically remove the streak along with the cosmic ray. However, in cases where an object of interest has been affected the user must be more careful. While standard techniques such as **wfixup** will interpolate across affected pixels and produce an acceptable cosmetic result, interpolation can bias both photometry and astrometry. In cases where accurate reconstruction of the true image is important, modelling of the charge transfer is required. For further information on charge traps, including the measured parameters of the larger traps, users should consult *WFPC2 ISR 95-02*, available on the WFPC2 web pages.



## Chapter 27

# WFPC2

# Error Sources

### In This Chapter...

Bias Subtraction Error / 27-2

Flatfield Correction Errors / 27-2

Dark Current Subtraction Errors / 27-3

Image Anomalies / 27-5

This chapter discusses some of the error sources associated with WFPC2 data. Most of the chapter focuses on specific calibration errors, complementing and partially overlapping the discussion given in “Post-Pipeline Calibration” on page 26-15. Other subtle errors and problems which appear in WFPC2 data, but which are not directly related to data calibration, are discussed at the end of this chapter and in Chapter 28.

Keep in mind that many of the error sources affecting calibrated WFPC2 data can be greatly reduced, or even corrected entirely, by either recalibration with newer calibration reference files or post-pipeline calibration. The routine pipeline calibration initially performed on a dataset before it is deposited in the Archive and delivered to the observer uses the most current, WFPC2-specific calibration reference files available at the time of processing. If there appear to be unusual features in the data, or if the analysis requires a high level of accuracy, it is important to determine if a better set of later calibration reference files can be used to recalibrate the data. Finding that a calibration reference file has changed since the data were calibrated doesn't always mean that recalibration is necessary. The decision to recalibrate depends very much on which calibration image or table changed, and whether that kind of correction is likely to affect the analysis. Chapter 26 gives more details on the required procedures.

---

## 27.1 Bias Subtraction Error

Very early on, it was discovered that the first few columns of the overscan region of WFPC2 CCDs, used for bias subtraction, can be positively offset if a strong signal is present in the image itself. The consequence was oversubtraction of the bias level. The sky background level in such images is incorrect, and in a few cases a significant part of the calibrated image has negative pixel values. The problem was fixed in **calwp2** version 1.3.0.5 (March 1994).

Slightly later, it was also realized that proper bias subtraction occasionally requires the use of separate bias values for odd and even columns. WFPC2 data taken before May 4, 1994 did not use this form of bias subtraction. As a result a striated pattern with a typical amplitude of a few electrons (a fraction of a DN) may remain in these images. These data will benefit from recalibration with **calwp2**, version 1.3.0.6 or later, unless the signal of the observation is so large that the noise statistics are dominated by Poisson noise. A recent study of the properties of bias frames throughout WFPC2 operations can be found in the *WFPC2 ISR 97-04*. From their results, it appears that large differences between the bias level in the even and odd columns have been rare after 1995, thus it is unlikely that recent WFPC2 data suffer from this problem to any measurable degree.

---

## 27.2 Flatfield Correction Errors

Early WFPC2 data were flattened using flatfields that did not take into account the large-scale structure of the flatfield. The offending flats have names that begin with “d” or “e1”.

Some special-purpose filters (such as the polarizers) did not have flats made until well after the installation of WFPC2. Some, such as the Woods filter (F160BW), still do not have an accurate flatfield. In these cases, the PEDIGREE and DESCRIP keywords for the flatfield file, reported at the end of the header of the calibrated image in HISTORY records, will indicate the existence of a problem at the time the data were taken. A pedigree of DUMMY indicates that the flatfield is identically 1, thus no real flatfield correction has been performed. A pedigree of GROUND indicates that the flatfield has been obtained purely from data taken during the pre-launch Thermal Vacuum test, and thus does not reflect properly the illumination function typical of the HST OTA; in this case, zonal errors of several percent can be encountered. Such cases are extremely rare after the summer of 1996, but are not uncommon for data taken in 1994 and early 1995, when the basic camera calibration was not yet completed.

A completely new generation of flatfields has been delivered between late 1995 (for the filters used in Hubble Deep Field observations) and 1996. These flatfields are more accurate than the previous ones, although few users will need to recalibrate as a result of this change. In the optical, the new flats differ from the old by 1% or less over the vast majority of the chip, with the differences growing

in the outer 50 pixels of the chip to about 8% at all wavelengths. Longward of 850 nm, differences of up to 1.5% are seen across the main body of the chips, and shortward of 300 nm the differences between the old and new flatfields are less than 3% over most of the chip.

WFPC2 flatfields are defined so that a source of constant brightness produces the same count rate per pixel across the image. However, due to geometric distortion of the image by the optics, the area of WFPC2 pixels on the sky depends on location on the chip. The total variation across the chip is a few percent. Therefore, the photometry of point sources is slightly corrupted by the standard flattening procedure. This effect, and its correction, are discussed in “Geometric Distortion” on page 28-12.

---

## 27.3 Dark Current Subtraction Errors

### 27.3.1 Electronic Dark Current

At the operating temperature of -88 C, maintained after April 23, 1994, the WFPC2 CCDs have a low dark background, ranging between 0.002 and 0.01  $e^-/s/pixel$ . A relatively small number of pixels have dark currents many times the value. These *warm pixels* are discussed in great detail in Chapter 26. To remove the dark current, the standard pipeline procedure takes a dark reference file (which contains the average dark background in DN/s), multiplies it by the dark time (determined by the header keyword DARKTIME), and subtracts this from the bias subtracted image. Prior to April 23, 1994, the CCDs were operated at -77 C. The correction procedure is the same for these early data, but the average dark current was about an order of magnitude higher due to the higher temperature. Hence, the dark current correction is both more important and less accurate than for later data.

The dark time is usually close to the exposure time, but it can exceed the latter substantially if the exposure was interrupted and the shutter closed temporarily, for example as a consequence of loss of lock. Such instances are rare and should be identified in their header keyword EXPFLAG and in the data quality comments for each observation, but will also be indicated by a difference between the exposure start and end time which is greater than the total exposure time. The true dark time differs slightly from pixel to pixel because of the different time elapsed between reset and readout. To the extent that dark current is constant with time, this small differential is present both in the bias image and in the observation itself, and therefore is automatically corrected by the bias subtraction.

New dark reference files are delivered on a weekly basis, but because of the necessary processing, they are usually available a week or two later than the observation itself. As a result, the dark used in the pipeline is not the same as the dark reference file recommended by StarView. The primary difference between successive darks is in the location and value of hot pixels. This difference will be most notable if a decontamination occurred between the images used to create the

dark and the observation itself. However, because direct treatment of the warm pixels themselves, rather than dark file subtraction, now appears the best way to remove warm pixels, many users will find that they do not need to reprocess with the most up-to-date dark file. For more details, see “Warm Pixels” on page 26-16.

Until August 1996, the weekly standard darks were based on a relatively small number (10) of exposures, taken over a time span of two weeks, in order to track the variable warm pixels. However, these darks can be a significant component of the total noise in deep images. Observers whose (pre-August 1996) images are formed from exposures totalling more than five orbits may therefore wish to recalibrate their data using the so-called *superdarks*, which have been generated by combining over 100 individual exposures (see the reference file memo on the WFPC2 Web page).

Since August 1996, the weekly standard darks have been produced by combining the relevant superdark with the warm pixel information in the dark frames taken that week. The combined file is obtained by using the superdark value for all pixels that appear normal in the weekly dark, namely, for which the dark current value in the weekly dark does not differ from the superdark value by more than  $3\sigma$ . For pixels that do deviate more than  $3\sigma$ , the weekly dark value is used. This compromise allows a timely tracking of warm pixels, while maintaining the low noise properties of the superdark for pixels that do not appear to change. Recalibration may still be appropriate, because the weekly standard dark is not yet available when the image is processed and archived at STScI.

### 27.3.2 Dark Glow

While the electronic dark current is relatively stable between observations, a component of the “dark current” has been seen to vary between observations. The intensity of this *dark glow* is correlated with the observed cosmic ray rate, and the glow is believed to be due to luminescence in the  $\text{MgF}_2$  CCD windows under cosmic ray bombardment. As a result of the geometry of the windows, the dark glow is not constant across the chip, but rather shows a characteristic edge drop of about 50%. The dark glow is significantly stronger in the PC, where it dominates the total dark background, and weakest in the WF2. The average *total* signal at the center of each camera is  $0.006\text{ e}^-/\text{s}$  in the PC,  $0.004\text{ e}^-/\text{s}$  in WF3 and WF4, and  $0.0025\text{ e}^-/\text{s}$  in WF2; of this, the true dark current is approximately  $0.0015\text{ e}^-/\text{s}$ , and the rest is dark glow. For more details, see the *WFPC2 Instrument Handbook*, Version 4.0, pages 71-75.

Because of the variability in the dark glow contribution, the standard dark correction may leave a slight curvature in the background. For the vast majority of observations, this is not a significant problem, because of the very low level of the error (worst-case center-to-edge difference of  $2\text{ e}^-/\text{pixel}$ ) and its slow variation across the chips. However, if an observation requires careful determination of the absolute background level, observers are encouraged to contact their WFPC2 contact scientist or the Help Desk ([help@stsci.edu](mailto:help@stsci.edu)).

## 27.4 Image Anomalies

In this section we present a number of unusual occurrences which occasionally affect WFPC2 data.

### 27.4.1 Bias Jumps

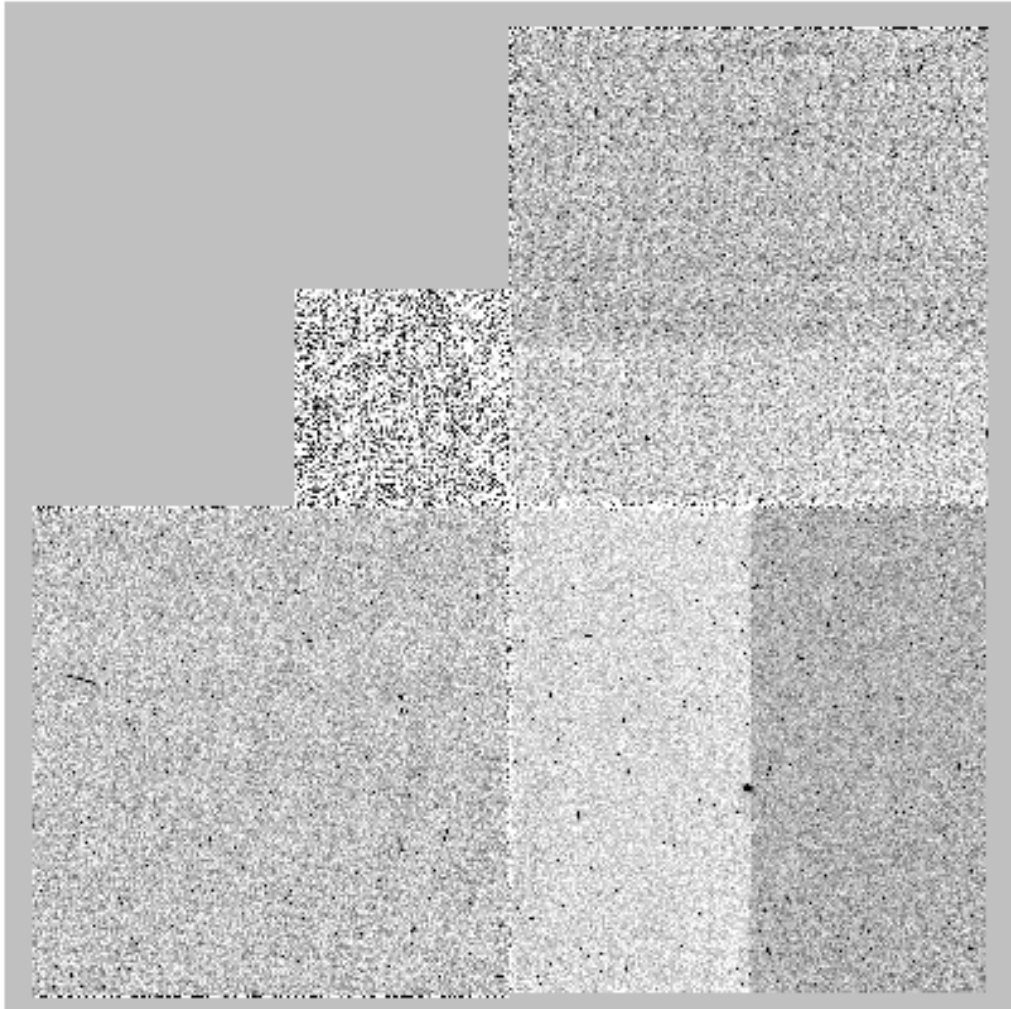
The average bias level for each image is obtained from the engineering data file (.x0h/.x0f) separately for even and odd columns. However, WFPC2 is subject to *bias jumps*, changes of the bias level during the readout. Large bias jumps (> 0.5 DN) are relatively rare, but small bias jumps, at the 0.1 DN level, affect about 10% of all images. Figure 27.1 shows a very unusual event where the bias has jumped in two chips during the same image.

Bias jumps are fairly obvious from a cursory inspection of the image, but users are alerted to their possible presence by a comment in the data quality file (suffix .pdq). Bias jumps are currently identified by an automatic procedure that searches the overscan data for possible anomalies; for details see *WFPC2 ISR 97-04*. Only jumps larger than 0.09 DN are reported. Prior to August 1996, the identification of bias jumps was done manually. Some of the bias jumps indicated in the data quality file are false positives, caused by image features, such as strongly saturated stars, which affect the overscan data.

There is no standard procedure to remove this defect, but it can be corrected by measuring the jump in the .x0h (bias) file or directly in the image if the image is clean enough. Standard IRAF procedures such as **imexamine** or **imstat** are sufficient to obtain a good estimate of the offset. The offset can then be removed, for instance, by subtracting the bias jump and then copying out the affected chip to another image, using the command:

```
im> imcalc image_in image_out "if (y.lt.YJUMP) then im1 \
>>> else (im1 - BJUMP)"
```

where YJUMP is the line at which the jump occurs, and BJUMP is its amplitude. The image `image_out` can then be copied back into the appropriate WFPC image group using the **imcopy** task.

**Figure 27.1:** Bias Jump in Two Chips

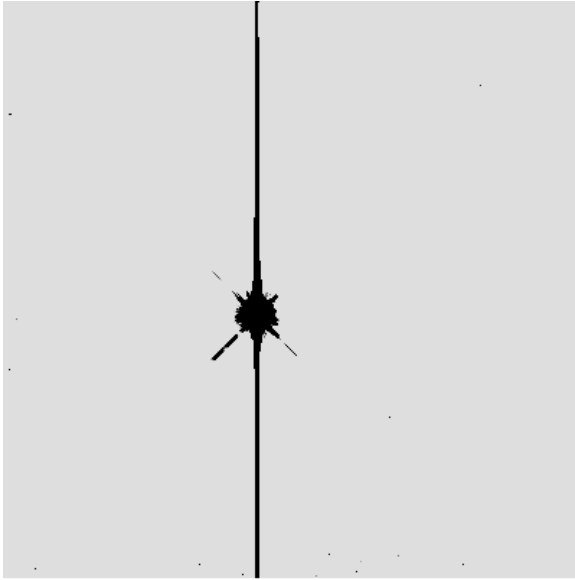
### 27.4.2 Residual Images

Observations of very bright sources can leave behind a residual image. This residual is caused by two distinct effects. In the first effect, charge in heavily saturated pixels is forced into deeper layers of the CCD which are not normally cleared by readout. Over time, the charge slowly leaks back into the imaging layers and appears in subsequent images. The time scale for leakage back into the imaging region depends on the amount of over-exposure. Strongly saturated images can require several hours to clear completely. The second effect is caused by charge transfer inefficiencies. At all exposure levels some charge becomes temporarily bound to impurities in the silicon of the CCD. The effect is most noticeable in images with high exposure levels, probably because electrons become exposed to more impurities as the wells are filled. This effect leaves behind charge both in bright regions of the image and in the part of the chip through which the bright objects were read out.

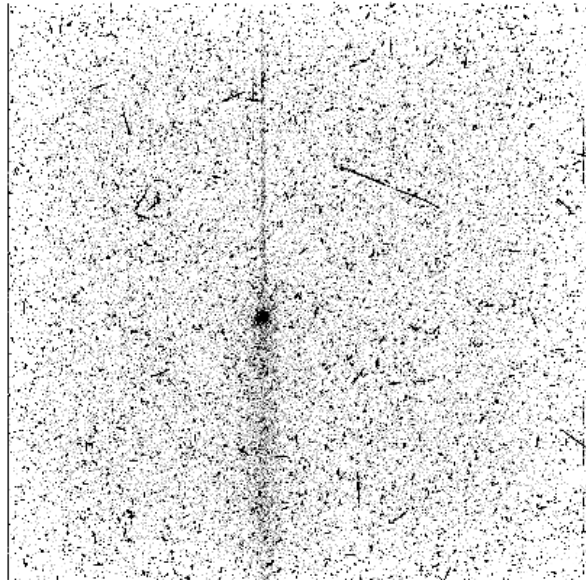
Figure 27.2 shows a saturated star on PC1 and the residual image seen in an 1800 second dark calibration frame which was started six minutes later. Note that the residual image is bright not only where the PC image was overexposed (effect 1), but also in a wide swath below the star due to the second effect and a narrower swath above the star due to bleeding during the exposure.

**Figure 27.2:** Saturated Star and Residual Image

**a) Saturated Star on PC1**



**b) Residual Image on Dark Frame 6 Minutes Later**

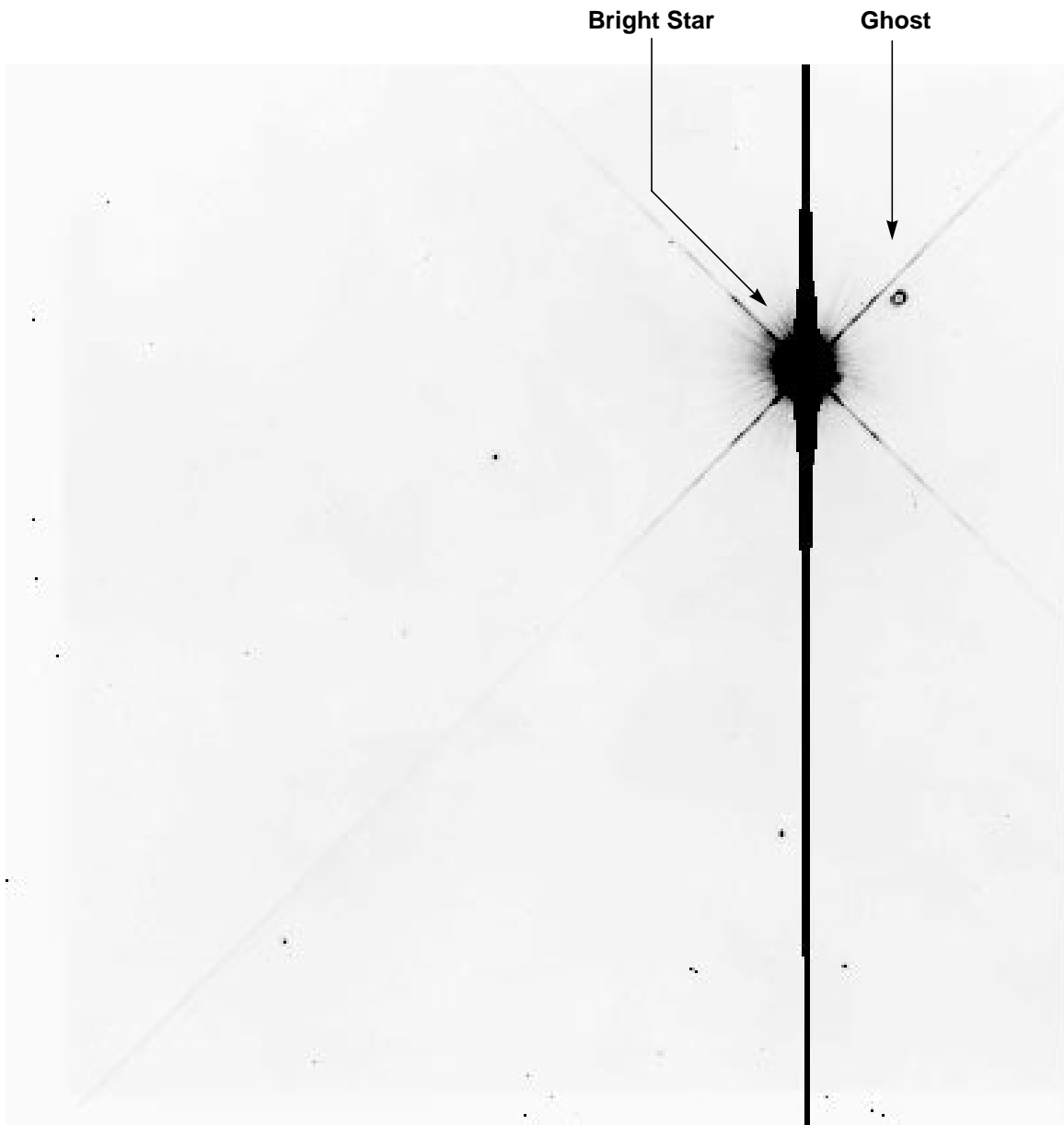


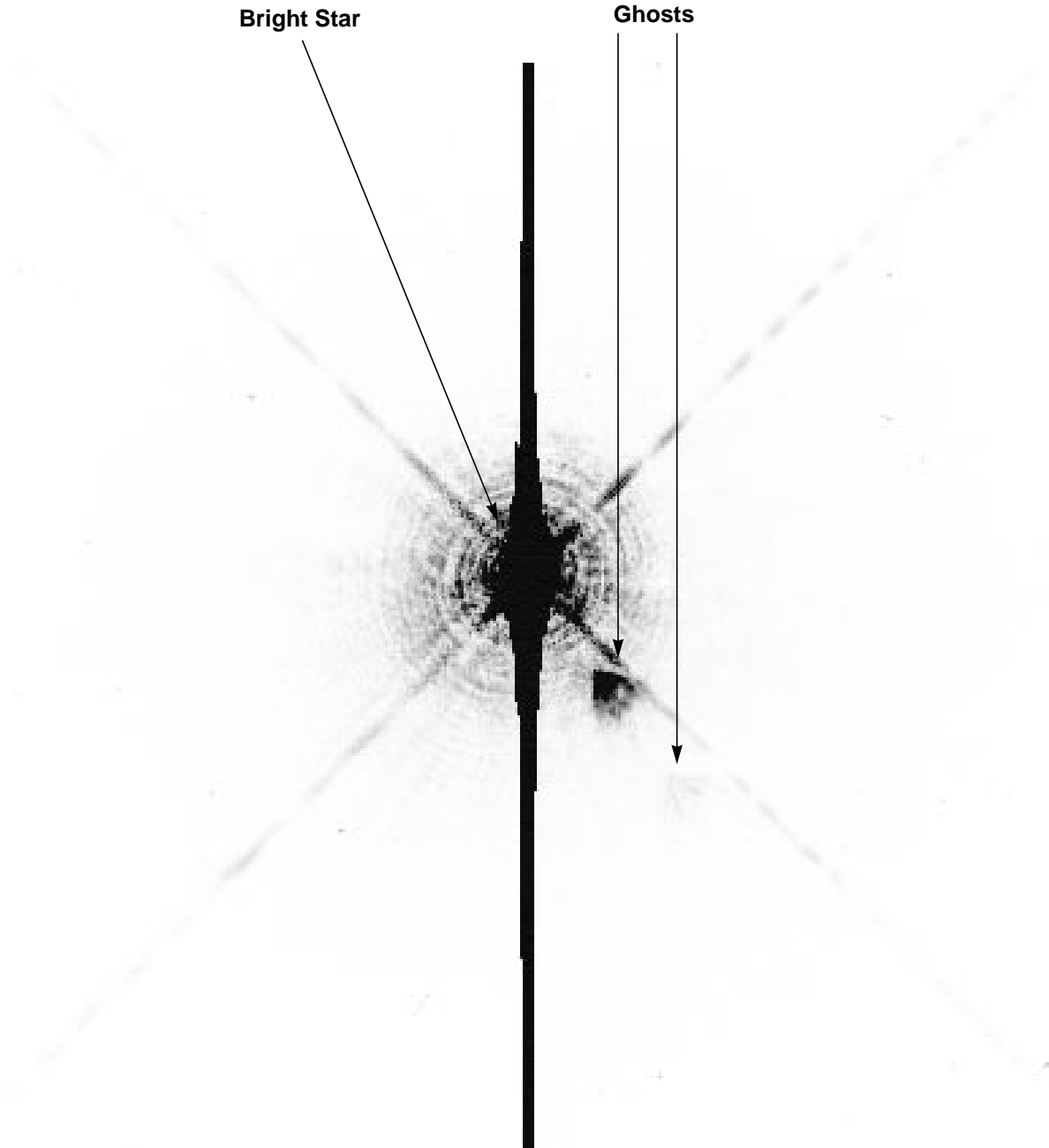
### Ghosts

Ghost images may occur on images of bright objects due to internal reflections in the WFPC2 camera. The most common ghosts are caused by internal reflections in the  $\text{MgF}_2$  field flatteners. In these ghosts, the line connecting the ghost and the primary image passes through the optical center of the chip. The ghost always lies further away from the center than the primary image. Figure 27.3 gives an example of one of these ghosts.

Ghosts may also occur due to reflections on the internal surfaces of a filter. The position of these ghosts will vary from filter to filter and chip to chip. For any given filter and chip combination, the direction of the offset of the ghost from the primary image will be constant, although the size of the offset may vary as a function of the position of the primary image. Filter ghosts can be easily recognized by their comatic (fan-shaped) structure. Particularly bright objects may produce multiple ghosts due to repeated internal reflections. Figure 27.4 shows an example of filter ghosts.

**Figure 27.3:** Field-Flattener Ghost in WF2—Image Shows Entire CCD



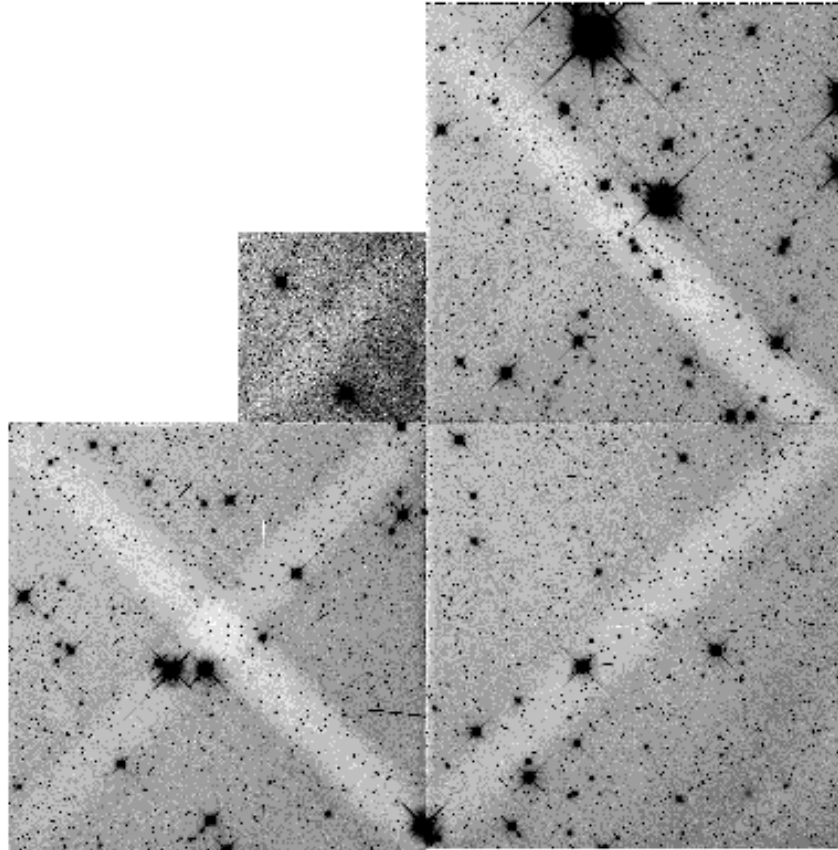
**Figure 27.4:** Detail of Filter Ghosts on WF4

### Earth Reflections

Light from the bright sun-lit Earth is on rare occasion reflected off the Optical Telescope Assembly (OTA) baffles and secondary support and into the WFPC2. These reflections can occur when the bright Earth is less than ~40 degrees from the OTA axis. (The default bright Earth limb avoidance is 20 degrees. Science observations are not scheduled at smaller limb angles to the sunlit Earth). The light raises the overall background level of the field; however, the WFPC2 camera mirror supports can vignette the scattered light, producing either X-shaped or

diagonal depressions in the level of the background. Figure 27.5 shows a typical example of the pattern formed by the scattered light. The scattered light in this image has a level of about 100 electrons. The darkest portion of the X is about 40 electrons below the average background level.

**Figure 27.5:** Scattered Light Pattern



### 27.4.3 PC1 Stray Light

The WFPC2 was originally intended to contain two separate pyramids—one for four PC cameras and the other for four WF cameras. Budget reductions caused the PC pyramid to be abandoned and the first WF camera to be replaced by a PC camera. However, the pyramid mirror corresponding to the PC camera was not reduced in size. As a result, baffling for the PC chip is not optimal, and a bright star falling on the pyramid outside of the PC field of view can produce an obvious artifact typically shaped like a broad, segmented arc. A star bright enough to produce a total count rate of 1 DN/s on the chip, will produce a ghost with a count rate of about  $1 \times 10^{-7}$  DN/pixel/s over the affected region. When scheduling observations, users should avoid placing stars brighter than  $V \sim 14$  in the L-shaped region surrounding the PC.

#### 27.4.4 Other Anomalies

Other image anomalies, such as bright streaks from other spacecraft, scattered light from bright stars near the field of view, and missing image sections due to dropped data occur on rare occasion. For more information, consult *WFPC2 ISR 95-06*, which can be obtained through the WFPC2 Web page or through the STScI Help Desk ([help@stsci.edu](mailto:help@stsci.edu)).



# WFPC2 Data Analysis

### In This Chapter...

Photometric Zero Point / 28-2
Photometric Corrections / 28-6
Polarimetry / 28-16
Astrometry / 28-18
Dithering / 28-19
Accuracy of WFPC2 Results / 28-23

This chapter deals with several topics pertaining to WFPC2 data analysis. We begin with a practical guide to photometry with WFPC2, in which we discuss how to accurately determine the zeropoint, photometric corrections that should be made to WFPC2 data, and common problems and their solutions. We start with the most important aspects of the photometric calibration that affect all observers, largely independently of the final accuracy desired, and in later sections consider subtle effects that can produce relatively small errors. A relatively simple calibration will produce photometric errors of 5 to 10%. With attention to more subtle effects, photometric accuracy between 2 and 5% can be achieved. We then discuss the analysis of polarization data, the astrometric characteristics of WFPC2 images, and the reconstruction of dithered data via the STSDAS package **dither**. Sub-pixel dithering is widely recognized—after the success of the Hubble Deep Field observations—as a valuable way to overcome in part the undersampling of WFPC2 images. Finally, we summarize various accuracies to be expected from well-calibrated WFPC2 observations.

Additional information on many WFPC2 data analysis topics can be found via the WFPC2 Clearinghouse. The Clearinghouse includes references to STScI documentation, publications from the astronomical literature, and user-submitted documentation, organized into more than 50 topics. The Clearinghouse can be found on the following web page:

[http://www.stsci.edu/ftp/instrument\\_news/WFPC2/Wfpc2\\_clear/wfpc2\\_clrhs.html](http://www.stsci.edu/ftp/instrument_news/WFPC2/Wfpc2_clear/wfpc2_clrhs.html)

## 28.1 Photometric Zero Point

The zero point of an instrument, by definition, is the magnitude of an object that produces one count (or data number, DN) per second. The magnitude of an arbitrary object producing DN counts in an observation of length EXPTIME is therefore:

$$m = -2.5 \times \log_{10}(\text{DN} / \text{EXPTIME}) + \text{ZEROPOINT}$$

It is the setting of the zeropoint, then, which determines the connection between observed counts and a standard photometric system (such as Cousins RI), and in turn between counts and astrophysically interesting measurements such as the flux incident on the telescope.

### Zero Points and Apertures

Each zero point refers to a count rate (DN/EXPTIME) measured in a specific way. The zeropoints published by Holtzman et al. (1995b) refer to counts measured in a standard aperture of 0.5" radius. The zeropoint derived from the PHOTFLAM header keyword, as well as in other STScI publications, refer—for historical continuity—to counts measured in an “infinite” aperture. Since it is not practical to measure counts in a very large aperture, we use a nominal infinite aperture, defined as having 1.096 times the flux in an aperture with 0.5" radius. This definition is equivalent to setting the aperture correction between 0.5" radius and infinite aperture to exactly 0.10 mag.

### 28.1.1 Photometric Systems Used for WFPC2 Data

There are several photometric systems commonly used for WFPC2 data, often causing some confusion about the interpretation of the photometric zeropoint used—and of the photometry results themselves. Before continuing with the discussion of the photometry, it is worthwhile to define these photometric systems more precisely.

The first, fundamental difference between systems has to do with the filter set on which they are based. The WFPC2 filters do not have exact counterparts in the standard filter sets. For example, while F555W and F814W are reasonable approximations of Johnson V and Cousins I respectively, neither match is exact, and the differences can amount to 0.1 mag—clearly significant in precise photometric work. Other commonly used filters, such as F336W and F606W, have much poorer matches in the Johnson-Cousins system. We recommend that, whenever practical, WFPC2 photometric results be referred to a system based on its own filters. It is possible to define “photometric transformations” to convert these photometry results to one of the standard systems; see Holtzman et al. (1995b) for some examples. However, such transformations have limited precision, depend on the color range, metallicity, and surface gravity of the stars considered, and can easily errors of 0.2 mag or more, depending on the filter and on how much the spectral energy distribution differs from that of the objects on which the transformation is defined; this happens frequently for galaxies at high redshift.

Two photometric systems based on WFPC2 filters are the WFPC2 flight system, defined by the WFPC2 IDT and detailed in Holtzman et al. (1995b), and the synthetic system, also defined by the IDT and subsequently used in **synphot** as the VEGAMAG system. For more references, see Harris et al. (1993), Holtzman et al. (1995b), *WFPC2 ISR 96-04*, and the *Synphot User's Guide*.

The WFPC2 flight system is defined so that stars of color zero in the Johnson-Cousins UBVRI system have color zero between any pair of WFPC2 filters, and have the same magnitude in V and F555W. This system was established by Holtzman et al. (1995b) by observing two globular cluster fields, in  $\omega$  Cen and in NGC 6752, with HST and from the ground; ground-based observations were taken both with WFPC2 flight-spare filters and with standard UBVRI filters. In practice, the system was defined by least-squares optimization of the transformation matrix. The stars near color zero which were observed are primarily white dwarfs, so the WFPC2 zeropoints defined in this system match the UBVRI zeropoints for stars with high surface gravity; the zeropoints for main sequence stars would be off by 0.02–0.05 mag, depending on the filter.

The zeropoints in the WFPC2 synthetic system, as defined in Holtzman et al. (1995b), are determined so that the magnitude of Vega, when observed through the appropriate WFPC2 filter, would be identical to the magnitude Vega has in the closest equivalent filter in the Johnson-Cousins system. For the filters in the photometric filter set, F336W, F439W, F555W, F675W, and F814W, these magnitudes are 0.02, 0.02, 0.03, 0.039, and 0.035, respectively. The calculations are done via synthetic photometry. In the **synphot** implementation, called the VEGAMAG system, the zeropoints are defined by the magnitude of Vega being *exactly* zero in all filters.

The above systems both tie the zeropoints to observed standards. In recent years, it has become increasingly common to use photometric systems in which the zeropoint is defined directly in terms of a reference flux in physical units. Such systems make the conversion of magnitudes to fluxes much simpler and cleaner, but have the side effect that any new determination of the absolute efficiency of the instrumental setup results in revised magnitudes. The choice between standard-based and flux-based systems is mostly a matter of personal preference.

The prevalent flux-based systems at UV and visible wavelengths are the AB system (Oke 1974) and the STMAG system. Both define an *equivalent flux density* for a source, corresponding to the flux density of a source of predefined spectral shape that would produce the observed count rate, and convert this equivalent flux to a magnitude. The conversion is chosen so that the magnitude in V corresponds roughly to that in the Johnson system. In the STMAG system, the flux density is expressed per unit *wavelength*, and the reference spectrum is flat in  $f_\lambda$ , while in the AB system, the flux density is expressed per unit *frequency*, and the reference spectrum is flat in  $f_\nu$ . The definitions are:

$$m_{AB} = -48.60 - 2.5 \log f_\nu$$

$$m_{ST} = -21.10 - 2.5 \log f_\lambda$$

where  $f_\nu$  is expressed in  $\text{erg cm}^{-2} \text{s}^{-1} \text{Hz}^{-1}$ , and  $f_\lambda$  in  $\text{erg cm}^{-2} \text{s}^{-1} \text{\AA}^{-1}$ .

Another way to express these zero points is to say that an object with  $f_V = 3.63 \cdot 10^{-20} \text{ erg cm}^{-2} \text{ s}^{-1} \text{ Hz}^{-1}$  will have  $m_{AB}=0$  in every filter, and an object with  $f_\lambda = 3.63 \cdot 10^{-9} \text{ erg cm}^{-2} \text{ s}^{-1} \text{ \AA}^{-1}$  will have  $m_{ST}=0$  in every filter. See also the discussion in the *Synphot User's Guide*.

## 28.1.2 Determining the Zero Point

There are several ways to determine the zero point, partly according to which photometric system is desired:

1. **Do it yourself:** Over the operational life of WFPC2, a substantial amount of effort has gone into obtaining accurate zeropoints for all of the filters used on HST. Nonetheless, if good ground-based photometry is available for objects in your HST field, it can be used to determine a zeropoint for these observations. This approach may be particularly useful in converting magnitudes to a standard photometric system, provided all targets have similar spectral energy distribution; in this case the conversions are likely to be more reliable than those determined by Holtzman et al (1995b), which are only valid for stars within a limited range of color, metallicity, and surface gravity.
2. **Use a summary list:** Lists of zeropoints have been published by Holtzman et al. (1995b), *WFPC2 ISR 96-04*, and *WFPC2 ISR 97-10* (also reported in Table 28.1). The Holtzman et al. (1995b) zeropoints essentially *define* the WFPC2 flight photometric system; as discussed above, they are based on observations of  $\omega$  Cen and NGC 6752 for the five main broad band colors (i.e., F336W, F439W, F555W, F675W, F814W), as well as synthetic photometry for most other filters. Transformations from the WFPC2 filter set to UBVRI are included, although these should be used with caution, as stated above. Holtzman et al. (1995b) also includes a cookbook section describing in detail how to do photometry with WFPC2. This paper is available from the STScI WWW or by sending e-mail to [help@stsci.edu](mailto:help@stsci.edu). The more recent compilations of zeropoints in *WFPC2 ISR 96-04* and *97-10* use new WFPC2 observations, are based on the VEGAMAG system, and do not include new conversions to UBVRI.
3. **Use the PHOTFLAM keyword in the header of your data:** The simplest way to determine the zeropoint of your data is to use the PHOTFLAM keyword in the header of your image. PHOTFLAM is the flux of a source with constant flux per unit wavelength (in  $\text{erg s}^{-1} \text{ cm}^{-2} \text{ \AA}^{-1}$ ) which produces a count rate of 1 DN per second. This keyword is generated by the synthetic photometry package **synphot**, which you may also find useful for a wide range of photometric and spectroscopic analyses. Using PHOTFLAM, it is easy to convert instrumental magnitude to flux density, and thus determine a magnitude in a flux-based system such as AB or STMAG (see previous Section); the actual steps required are detailed below.



Note that the zeropoints listed by Holtzman et al. (1995b) differ systematically by 0.85 mag from the **synphot** zeropoints in Table 28.1. Most of the difference, 0.75 mag, is due to the fact that the Holtzman zeropoints are given for gain 14, while the **synphot** zeropoints are reported for gain 7, which is generally used for science observations. An additional 0.1 mag is due to the aperture correction: the Holtzman zeropoint refers to an aperture of 0.5", while the **synphot** zeropoint refers to a *nominal* infinite aperture, defined as 0.10 mag brighter than the 0.5" aperture.

The tables used by the **synphot** package were updated in August 1995 and May 1997. With these updates, **synphot** now provides absolute photometric accuracy of 2% rms for broad-band and intermediate-width filters between F300W and F814W, and of about 5% in the UV. Narrow-band filters are calibrated using continuum sources, but checks on line sources indicate that their photometric accuracy is also determined to 5% or better (the limit appears to be in the quality of the ground-based spectrophotometry). Prior to the May 1997 update, some far UV and narrow-band filters were in error by 10% or more; more details are provided in *WFPC2 ISR 97-10*.

Table 28.1 lists the new values for PHOTFLAM. Please note that the headers of images processed before May 1997 contain out-of-date values of PHOTFLAM; the up-to-date values can be obtained by reprocessing the image, from the table, or more directly, by using the **bandpar** task in **synphot**—as long as the **synphot** version is up to date.<sup>1</sup> When using **bandpar**, it is also possible to incorporate the contamination correction (see “Contamination” on page 28-6) directly into the value of PHOTFLAM.

The **synphot** package can be used to determine the transformation between magnitudes in different filters, subject to the uncertainties related to how well the spectrum chosen to determine the transformation matches the spectrum of the actual source. The transformation is relatively simple using **synphot**, and the actual correction factors are small when converting from the WFPC2 photometric filter set to Johnson-Cousins magnitudes. For example, the following commands can be used to determine the difference in zeropoint between F814W filter and the Cousins I band for a K0III star on WF3 using the gain=7 setting:

```
sy> calcpHOT "band(wfpc2,3,a2d7,f814W)" crgridbz77$bz_54 stmag
where the Bruzual stellar atlas is being used to provide the spectrum for the K0 III
star (file = crgridbz77$bz_54). The output is:

sy> calcpHOT "band(wfpc2,3,a2d7,f814W)" crgridbz77$bz_54 stmag
Mode = band(wfpc2,3,a2d7,f814W)
      Pivot      Equiv Gaussian
Wavelength      FWHM
      7982.044      1507.155      band(wfpc2,3,a2d7,f814W)
Spectrum: crgridbz77$bz_54
```

1. For instructions on how to retrieve STSDAS **synphot** tables, see “Getting the Synphot Database” on page A-15.

```
VZERO          STMAG      Mode: band(wfpc2,3,a2d7,f814W)
0.             -15.1045
```

Comparing this result with:

```
calcpHOT "band(cousins,I)" crgridbz77$bz_54 vegamag
Mode = band(cousins,I)
  Pivot      Equiv Gaussian
Wavelength   FWHM
7891.153     898.879   band(cousins,I)
Spectrum: crgridbz77$bz_54
  VZERO      VEGAMAG    Mode: band(cousins,I)
0.          -16.3327
```

shows that for a star of this color, the correction is 1.3 magnitudes (note that nearly all of this offset is due to the definition of STMAG; the F814W filter is a very close approximation to the Johnson-Cousins I, and color terms between these filters are very small). More details on the use of **synphot** can be found in the *Synphot User's Guide*.

---

## 28.2 Photometric Corrections

A number of corrections must be made to WFPC2 data to obtain the best possible photometry. Some of these, such as the corrections for UV throughput variability, are *time dependent*, and others, such as the correction for the geometric distortion of WFPC2 optics, are *position dependent*. Finally, some general corrections are needed as part of the analysis process, such as the aperture correction. We describe each class in turn.

### 28.2.1 Time-Dependent Corrections

The most important time-dependent correction is that for the contamination of the CCD windows, which affects primarily UV observations. Other time-dependent corrections are due to the change in operating temperature in April 1994 and to the variations of the PSF with focus position; the latter is also position-dependent (see “Aperture Correction” on page 28-13 for more information).

#### Contamination

Contaminants adhere to the cold CCD windows of the WFPC2. Although these typically have little effect upon the visible and near infrared performance of the cameras, the effect upon the UV is quite dramatic, and can reduce throughput by about 30% after 30 days for the F160BW filter. These contaminants are largely removed during periodic warmings of the camera and fortunately, in between these decontaminations, the effect upon photometry is both linear and stable, and can be removed using values regularly measured in the WFPC2 calibration program. Table 28.2 shows the contamination rates measured for each detector and Table 28.3 provides decontamination dates up until August 1997. Updated lists are kept on the WFPC2 WWW pages.

**Table 28.1:** Current Values of PHOTFLAM and Zeropoint in VEGAMAG system

Filter <sup>a</sup>	PC		WF2		WF3		WF4	
	New photflam	Vega ZP						
F122M	8.088e-15	13.768	7.381e-15	13.868	8.204e-15	13.752	8.003e-15	13.778
F160BW	5.212e-15	14.985	4.563e-15	15.126	5.418e-15	14.946	5.133e-15	15.002
F170W	1.551e-15	16.335	1.398e-15	16.454	1.578e-15	16.313	1.531e-15	16.350
F185W	2.063e-15	16.025	1.872e-15	16.132	2.083e-15	16.014	2.036e-15	16.040
F218W	1.071e-15	16.557	9.887e-16	16.646	1.069e-15	16.558	1.059e-15	16.570
F255W	5.736e-16	17.019	5.414e-16	17.082	5.640e-16	17.037	5.681e-16	17.029
F300W	6.137e-17	19.406	5.891e-17	19.451	5.985e-17	19.433	6.097e-17	19.413
F336W	5.613e-17	19.429	5.445e-17	19.462	5.451e-17	19.460	5.590e-17	19.433
F343N	8.285e-15	13.990	8.052e-15	14.021	8.040e-15	14.023	8.255e-15	13.994
F375N	2.860e-15	15.204	2.796e-15	15.229	2.772e-15	15.238	2.855e-15	15.206
F380W	2.558e-17	20.939	2.508e-17	20.959	2.481e-17	20.972	2.558e-17	20.938
F390N	6.764e-16	17.503	6.630e-16	17.524	6.553e-16	17.537	6.759e-16	17.504
F410M	1.031e-16	19.635	1.013e-16	19.654	9.990e-17	19.669	1.031e-16	19.634
F437N	7.400e-16	17.266	7.276e-16	17.284	7.188e-16	17.297	7.416e-16	17.263
F439W	2.945e-17	20.884	2.895e-17	20.903	2.860e-17	20.916	2.951e-17	20.882
F450W	9.022e-18	21.987	8.856e-18	22.007	8.797e-18	22.016	9.053e-18	21.984
F467M	5.763e-17	19.985	5.660e-17	20.004	5.621e-17	20.012	5.786e-17	19.980
F469N	5.340e-16	17.547	5.244e-16	17.566	5.211e-16	17.573	5.362e-16	17.542
F487N	3.945e-16	17.356	3.871e-16	17.377	3.858e-16	17.380	3.964e-16	17.351
F502N	3.005e-16	17.965	2.947e-16	17.987	2.944e-16	17.988	3.022e-16	17.959
F547M	7.691e-18	21.662	7.502e-18	21.689	7.595e-18	21.676	7.747e-18	21.654
F555W	3.483e-18	22.545	3.396e-18	22.571	3.439e-18	22.561	3.507e-18	22.538
F569W	4.150e-18	22.241	4.040e-18	22.269	4.108e-18	22.253	4.181e-18	22.233
F588N	6.125e-17	19.172	5.949e-17	19.204	6.083e-17	19.179	6.175e-17	19.163
F606W	1.900e-18	22.887	1.842e-18	22.919	1.888e-18	22.896	1.914e-18	22.880
F622W	2.789e-18	22.363	2.700e-18	22.397	2.778e-18	22.368	2.811e-18	22.354
F631N	9.148e-17	18.514	8.848e-17	18.550	9.129e-17	18.516	9.223e-17	18.505
F656N	1.461e-16	17.564	1.410e-16	17.603	1.461e-16	17.564	1.473e-16	17.556
F658N	1.036e-16	18.115	9.992e-17	18.154	1.036e-16	18.115	1.044e-16	18.107
F673N	5.999e-17	18.753	5.785e-17	18.793	6.003e-17	18.753	6.043e-17	18.745
F675W	2.899e-18	22.042	2.797e-18	22.080	2.898e-18	22.042	2.919e-18	22.034
F702W	1.872e-18	22.428	1.809e-18	22.466	1.867e-18	22.431	1.883e-18	22.422
F785LP	4.727e-18	20.688	4.737e-18	20.692	4.492e-18	20.738	4.666e-18	20.701
F791W	2.960e-18	21.498	2.883e-18	21.529	2.913e-18	21.512	2.956e-18	21.498
F814W	2.508e-18	21.639	2.458e-18	21.665	2.449e-18	21.659	2.498e-18	21.641
F850LP	8.357e-18	19.943	8.533e-18	19.924	7.771e-18	20.018	8.194e-18	19.964
F953N	2.333e-16	16.076	2.448e-16	16.024	2.107e-16	16.186	2.268e-16	16.107
F1042M	1.985e-16	16.148	2.228e-16	16.024	1.683e-16	16.326	1.897e-16	16.197

a. Values are for the gain 7 setting. The PHOTFLAM values for gain 14 can be obtained by multiplying by the gain ratio: 1.987 (PC1), 2.003 (WF2), 2.006 (WF3), and 1.955 (WF4) (values from Holtzman et al. 1995b). For the zeropoints, add  $-2.5 \log(\text{gain ratio})$ , or  $-0.745$ ,  $-0.754$ ,  $-0.756$ , and  $-0.728$ , respectively. The above values should be applied to the counts referenced to a nominal "infinite aperture", defined by an aperture correction of 0.10 mag with respect to the standard aperture with 0.5" radius.

Contamination is measured primarily from the bimonthly observations of the WFPC2 primary standard, the white dwarf GRW+70d5824; thus the contamination rates in Table 28.2 are directly applicable to blue objects. These observations have been supplemented, for the standard photometric filters, by observations of a stellar field in the globular cluster  $\omega$  Cen (mean B–V  $\sim$  0.7 mag); the contamination rates thus measured (in parentheses in Table 28.2) are generally in good agreement with those measured on GRW+70d5824. The  $\omega$  Cen data also indicate a slightly higher contamination rate towards the center of each chip. For more details, see *WFPC2 ISR 96-04*. These results will be verified further with the analysis of UV observations of NGC 2100, a young globular cluster in the LMC.

The **synphot** package can be used to determine the effect of contamination on your observations. For example, the following command computes the expected countrate for a WF3, F218W observation taken 20 days (MJD=49835.0) after the April 8, 1995, decontamination, with the gain=7 setup:

```
sy> calcphot "wfpc2,3,f218w,a2d15,cont#49835.0" \
>>> spec="bb(8000)" form=counts
```

Removing the `cont#49835.0` from the command will determine the countrate if no contamination was present. An 8000 K black body spectrum was chosen largely as a matter of simplicity—the correction values for contamination depend only on the filter chosen and do not reflect the source spectrum.

**Table 28.2:** Contamination Rates (Fractional Loss per Day)

Filter	PC1	+/-	WF2	+/-	WF3	+/-	WF4	+/-
F160BW	-0.263	0.030	-0.378	0.090	-0.393	0.051	0.381	0.066
F170W	-0.160	0.011	-0.284	0.005	-0.285	0.006	-0.232	0.006
F218W	-0.138	0.009	-0.226	0.015	-0.255	0.010	-0.213	0.033
F255W	-0.070	0.007	-0.136	0.017	-0.143	0.009	-0.108	0.042
F336W	-0.016 (-0.038)	0.008 (0.018)			-0.057 (-0.046)	0.011 (0.008)		
F439W	-0.002 (0.002)	0.007 (0.014)			-0.021 (-0.023)	0.010 (0.009)		
F555W	-0.014 (0.007)	0.006 (0.013)			-0.016 (-0.009)	0.008 (0.009)		
F675W	-0.001 (-0.020)	0.006 (0.020)			-0.001 (0.002)	0.006 (0.011)		
F814W	0.007 (0.013)	0.007 (0.019)			0.003 (-0.000)	0.008 (0.009)		

**Table 28.3:** Dates of WFPC2 Decontaminations through August 1997<sup>a</sup>

Year.Day:Hour :Min	Day-Month- Year	Modified Julian Date	Year.Day:Hour: Min	Day-Month- Year	Modified Julian Date
1994.053:11:37	22-Feb-1994	49405.4840	1996.042:00:30	11-Feb-1996	50124.0208
1994.083:11:08	24-Mar-1994	49435.4639	1996.070:00:21	10-Mar-1996	50152.0147
1994.114:00:49	24-Apr-1994	49466.0340	1996.093:00:16	02-Apr-1996	50175.0111
1994.143:15:00	23-May-1994	49495.6250	1996.125:17:09	04-May-1996	50207.7146
1994.164:11:02	13-Jun-1994	49516.4597	1996.149:06:16	28-May-1996	50231.2614
1994.191:11:40	10-Jul-1994	49543.4861	1996.174:22:15	22-Jun-1996	50256.9277
1994.209:07:12	28-Jul-1994	49561.3000	1996.210:13:34	28-Jul-1996	50292.5653
1994.239:09:46	27-Aug-1994	49591.4069	1996.236:10:10	23-Aug-1996	50318.4242
1994.268:00:46	25-Sep-1994	49620.0319	1996.262:16:25	18-Sep-1996	50344.6840
1994.294:00:41	21-Oct-1994	49646.0285	1996.292:07:46	18-Oct-1996	50374.3236
1994.323:17:29	19-Nov-1994	49675.7285	1996.317:09:40	12-Nov-1996	50399.4031
1994.352:06:00	18-Dec-1994	49704.2500	1996.350:00:00	15-Dec-1996	50432.0417
1995.013:16:14	13-Jan-1995	49730.6764	1996.354:12:33	19-Dec-1996	50436.5229
1995.043:01:54	12-Feb-1995	49760.0792	1997.007:23:41	07-Jan-1997	50455.9875
1995.070:14:30	11-Mar-1995	49787.6042	1997.040:00:00	09-Feb-1997	50488.0006
1995.098:10:29	08-Apr-1995	49815.4368	1997.054:19:08	23-Feb-1997	50502.7978
1995.127:01:13	07-May-1995	49844.0507	1997.058:06:31	27-Feb-1997	50506.2721
1995.153:18:30	02-Jun-1995	49870.7708	1997.063:10:16	04-Mar-1997	50511.4278
1995.178:20:00	27-Jun-1995	49895.8333	1997.080:03:35	21-Mar-1997	50528.1494
1995.211:08:50	30-Jul-1995	49928.3681	1997.095:08:50	05-Apr-1997	50543.3681
1995.239:05:43	27-Aug-1995	49956.2382	1997.115:23:00	25-Apr-1997	50563.9583
1995.265:03:40	22-Sep-1995	49982.1528	1997.135:20:18	15-May-1997	50583.8460
1995.290:09:43	17-Oct-1995	50007.4053	1997.158:13:06	07-Jun-1997	50606.5461
1995.319:08:53	15-Nov-1995	50036.3706	1997.175:11:04	24-Jun-1997	50623.4612
1995.348:07:03	14-Dec-1995	50065.2929	1997.205:18:42	24-Jul-1997	50653.7795
1996.011:23:24	11-Jan-1996	50093.9750	1997.232:02:17	20-Aug-1997	50680.0952

a. The updated list of decontamination dates can be found on the World Wide Web at:

[http://www.stsci.edu/ftp/instrument\\_news/WFPC2/Wfpc2\\_memos/wfpc2\\_decon\\_dates.html](http://www.stsci.edu/ftp/instrument_news/WFPC2/Wfpc2_memos/wfpc2_decon_dates.html)

### Cool Down on April 23, 1994

The temperature of the WFPC2 was lowered from  $-76$  C to  $-88$  C on April 23, 1994, in order to minimize the CTE problem. While this change increased the contamination rates (see above), it also improved the photometric throughput, especially in the UV, and greatly reduced the impact of warm pixels. Table 28.4 provides a partial list of corrections to Table 28.1 for the pre-cool down throughput. Including the MJD in a **synphot** calculation using up-to-date tables will automatically provide an estimate of PHOTFLAM corrected for this change.

**Table 28.4:** Ratio Between Pre- and Post-Cool Down Throughput

Filter	PC	PC (mag)	WF	WF (mag)
F160BW	0.865	-0.157	0.895	-0.120
F170W	0.910	-0.102	0.899	-0.116
F218W	0.931	-0.078	0.895	-0.120
F255W	0.920	-0.091	0.915	-0.096
F336W	0.969	-0.034	0.952	-0.053
F439W	0.923	-0.087	0.948	-0.058
F555W	0.943	-0.064	0.959	-0.045
F675W	0.976	-0.026	0.962	-0.042
F814W	0.996	-0.004	0.994	-0.007

### PSF Variations

The point spread function (PSF) of the telescope varies with time, and these variations can affect photometry that relies on very small apertures and PSF fitting. Changes in focus are observed on an orbital timescale due to thermal *breathing* of the telescope and due to desorption, which causes a continual creeping of the focal position. This change has been about 0.7  $\mu\text{m}$  per month until mid-1996, when it greatly slowed. Currently the focus drift is less than 0.3  $\mu\text{m}$  per month. The effect of focus position on aperture photometry is described in *WFPC2 ISR 97-01*. About twice a year, the focal position of the telescope is moved by several microns to remove the effect of the desorption.

In addition, *jitter*, or pointing motion, can occasionally alter the effective PSF. The Observatory Monitoring System (OMS) files provide information on telescope jitter during observations (see Appendix C). These files are now regularly provided to the observer with the raw data. Observations taken after October 1994 have jitter files in the Archives. Limited requests for OMS files for observations prior to October 1994 can be handled by the STScI Help Desk (E-mail [help@stsci.edu](mailto:help@stsci.edu)).

Recently, Remy et al. (1997) have been able to obtain high-quality photometry of well-exposed point sources by modeling the point spread function with TinyTim (Krist, 1995), and taking into account focus and jitter terms via a chi-squared minimization method. Similar results have been obtained using observed PSFs (Surdej et al., 1997), provided that the PSF used is less than 10" from the observed star and corresponds to a spectral energy distribution similar to that of the target. The WFPC2 PSF library was established to help users find suitable PSFs, if they exist, or carry out experiments with what is available. The PSF library is described in Wiggs et al. (1997) and can be found at the following URL:

[http://www.stsci.edu/ftp/instrument\\_news/WFPC2/Wfpc2\\_psf/wfpc2-psf-form.html](http://www.stsci.edu/ftp/instrument_news/WFPC2/Wfpc2_psf/wfpc2-psf-form.html)

## 28.2.2 Position-Dependent Corrections

In this Section we discuss the CTE correction and the possibly related long vs. short anomaly, the geometric distortion, the gain differences between different chips, and the effect of pixel centering.

### Charge Transfer Efficiency

Shortly after launch it was discovered that WFPC2 had a substantial charge transfer efficiency (CTE) problem: objects appeared to be about 10% fainter when observed at the top of the chip ( $y \sim 800$ ) compared to when they were observed at the bottom of the chip ( $y \sim 0$ ). The April 23, 1994, cool down reduced the CTE problem to about a 4% effect peak-to-peak (Holtzman et al., 1995b) for a typical observation. The effect appears to be smaller, or nonexistent, in the presence of a moderate background.

Extensive observations made during Cycles 5 and 6 gave a much better characterization of the CTE calibration, indicating that its effect can be 5% or more (peak-to-peak) for faint images. *WFPC2 ISR 97-08* quantifies the CTE effect under various observational circumstances and gives empirical rules to correct for it. After these corrections, the residual CTE effect for well-exposed stars is estimated to be less than 2%.

The correction depends on the average background, the average counts over the chip, and the counts in the source itself. Assuming a 2 pixel aperture, the corrected counts are given by:

$$counts_{corrected} = \left[ 1 + \frac{Y-CTE}{100} \times \frac{Y}{800} + \frac{X-CTE}{100} \times \frac{X}{800} \right] counts_{observed}$$

where  $X$  and  $Y$  are the coordinates of the star center in pixels, and  $X-CTE$  and  $Y-CTE$  are the percentile loss over 800 pixels in the  $x$  and  $y$  direction, respectively, given by:

$$Y-CTE = 10^{(0.7994 - 0.2564 \times \log_{10} BKG_{blank}) + (0.2478 - 0.0987 \log_{10} counts_{observed})}$$

and

$$X-CTE = 7.373 - 1.57 \times \log_{10}(counts_{observed})$$

Here,  $BKG_{blank}$  is the mean number of counts in DN for a blank region of the sky. For more details and other correction formulae, see *WFPC2 ISR 97-08*.

### Long vs. Short Anomaly (non-linearity)

A comparison of repeated images of the same stellar field indicates that the count rates for the faint stars are higher for longer exposures. This apparent non-linearity appears to be a function of total counts in each source, rather than of count rates, and may depend on the image background. The magnitude errors produced appear to be less than 1% for well-exposed stars (over 30,000  $e^-$ ), but can rise to as much as 15% for faint stars (less than 300  $e^-$ ).<sup>2</sup> The effect is

2. See Casertano (1997), and Trauger (1997).

quantitatively similar to a loss of about 2 to 3  $e^-$  per pixel in an aperture with a radius of 2 to 5 pixels. Although there is no evidence that this apparent non-linearity is, strictly speaking, position-dependent, it may be closely related to the CTE loss, and thus the two are often studied together.

An extensive program of observations is planned for Cycle 7 to characterize this non-linearity more completely. A preliminary report, based on data from Cycles 4 and 5, is available at:

[http://www.stsci.edu/ftp/instrument\\_news/WFPC2/Wfpc2\\_cte/ctetop.html](http://www.stsci.edu/ftp/instrument_news/WFPC2/Wfpc2_cte/ctetop.html)

### Geometric Distortion

Geometric distortion near the edges of the chips results in a change of the surface area covered by each pixel. The flatfielding corrects for this distortion so that surface photometry is unaffected. However, integrated point-source photometry using a fixed aperture *will* be affected by 1 to 2% near the edges, with a maximum of about 4-5% in the corners. A correction image has been produced and is available from the Archive (f1k1552bu.r9h). The counts measured for a star centered at a given pixel position must be multiplied by the value of this image. A small residual effect, due to the fact that the aperture radius differs from the nominal size, depends on the aperture used and is generally well below 1%.

### Gain Variation

The absolute sensitivities of the four chips differ somewhat. Flatfields have been determined using the gain=14 setup, normalized to 1.0 over the region [200:600,200:600]. However, most science observations are taken using the gain=7 setup. Because the gain ratio varies slightly from chip to chip, PHOTFLAM values will be affected. The count ratios for the different chips from Holtzman (1995b) are:

- **PCI**: 1.987
- **WF2**: 2.003
- **WF3**: 2.006
- **WF4**: 1.955

These count ratios should be included in the zeropoint calculation if using values from Holtzman et al. (1995b) on gain=7 data. Conversely, their reciprocals should be applied when using **synphot** zeropoints on gain=14 data. If you use the value of PHOTFLAM from the header to determine your zeropoint, the different gains for the different chips will already be included. Remember to use the new PHOTFLAM values provided in Table 28.1 or the post-May 1997 **synphot** tables; those included in the header for data taken before May 1997 will have less accurate values.

### Pixel Centering

Small, sub-pixel variations in the quantum efficiency of the detector could affect the photometry. The position of star relative to the sub-pixel structure of the chip is estimated to have an effect of less than 1% on the photometry. At present there is no way to correct for this effect.

## 28.2.3 Other Photometric Corrections

Miscellaneous corrections that must be taken into account include: aperture corrections, color terms if transforming to non-WFPC2 filters, digitization noise and its impact on the estimate of the sky background, the effect of red leaks and charge traps, and the uncertainty of exposure times on short exposures taken with serial clocks on.

### Aperture Correction

It is difficult to measure directly the total magnitude of a point source with the WFPC2 because of the extended wings of the PSF, scattered light, and the small pixel size. One would need to use an aperture far larger than is practical. A more accurate method is to measure the light within a smaller aperture and then apply an offset to determine the total magnitude. Typically, magnitudes will be measured in a small aperture well-suited to the data at hand—a radius of 2–4 pixels, with a background annulus of 10–15 pixels, has been found adequate for data without excessive crowding—and the results corrected to the aperture for which the zeropoint is known. The aperture correction can often be determined from the data themselves, by selecting a few well-exposed, isolated stars. If such are not available, encircled energies and aperture corrections have been tabulated by Holtzman et al. (1995a). If PSF fitting is used, then the aperture correction can be evaluated directly on the PSF profile used for the fitting.

For very small apertures (1–2 pixels), the aperture correction can be influenced by the HST focus position at the time of the observation. The secondary mirror of HST is known to drift secularly towards the primary and to move slightly on time scales of order of an orbit. The secular shift is corrected by biannual moves of the secondary mirror, but the net consequence of this motion is that WFPC2 can be out of focus by up to 3–4  $\mu\text{m}$  of secondary mirror displacement at the time of any given observation. This condition affects the encircled energy at very small radii, and thus the aperture corrections, by up to 10% in flux (for 1 pixel aperture in the PC); see *WFPC2 ISR 97-01* for more details. If the use of very small apertures is required—because of crowding, S/N requirements, or other reasons—users are strongly advised to determine the aperture correction from suitable stars in their images. If such are not available, an *approximate* aperture-focus correction can be obtained as described in *WFPC2 ISR 97-01*.

A standard aperture radius of 0."5 has been adopted by Holtzman et al. (1995b) (note that Holtzman et al. 1995a used a radius of 1."0). For historic consistency, the WFPC2 group at STScI and the **synphot** tasks in STSDAS refer all measurements to the total flux in a hypothetical infinite aperture. In order to avoid uncertain correction to such apertures, both in calibration and in science data, this infinite aperture is *defined* by an aperture correction of exactly 0.10 mag with respect to the standard 0."5 aperture. Equivalently, the *total* flux is defined as 1.096 times the flux in the standard aperture of 0."5 radius. In practice, this means that observers wishing to use our tables or the **synphot** zero points should:

1. Correct the measured flux to a 0."5 radius aperture.
2. Apply an additional aperture correction of –0.10 mag (equivalently, multiply the flux by 1.096).

### 3. Determine the magnitude using the zeropoints given.

See also the example in “An Example of Photometry with WFPC2” on page 28-15.

### Color Terms

In some cases it may be necessary to transform from the WFPC2 filter set to more conventional filters (e.g., Johnson UBV or Cousins RI) in order to make comparisons with other datasets. The accuracy of these transformations is determined by how closely the WFPC2 filter matches the conventional filter and by how closely the spectral type (e.g., color, metallicity, surface gravity) of the object matches the spectral type of the calibration observations. Accuracies of 1–2% are typical for many cases, but much larger uncertainties are possible for certain filters (e.g., F336W with a red leak, see below), and for certain spectral types (e.g., very blue stars). Transformations can be determined by using **synphot**, or by using the transformation coefficients in Holtzman et al. (1995b).

### Digitization Noise

The minimum gain of the WFPC2 CCDs,  $7 e^-/ADU$ , is larger than the read noise of the chip. As a result, digitization can be a source of noise in WFPC2 images. This effect is particularly pernicious when attempting to determine sky values, because the measured values tend to cluster about a few integral values (dark subtraction and flatfielding cause the values to differ by slightly non-integral amounts). As a result, using a median filter to remove objects that fall within the background annulus in crowded fields, can cause a substantial systematic error, whose magnitude will depend on the annulus being measured. It is generally safer to use the mean, though care must then be taken to remove objects in the background annulus.

A more subtle effect is that some statistics programs assume Gaussian noise characteristics when computing properties such as the median and mode. Quantized noise can have surprising effects on these programs. The recommended strategies for sky determination are described in *WFPC2 ISR* 96-03.

### Red Leaks

Several of the UV filters have substantial red leaks that can affect the photometry. For example, the U filter (F336W) has a transmission at  $7500 \text{ \AA}$  that is only about a factor of 100 less than at the peak transmission at about  $3500 \text{ \AA}$ . The increased sensitivity of the CCDs in the red, coupled with the fact that most sources are brighter in the red, makes this an important problem in many cases. The **synphot** tasks can be used to estimate this effect for any given source spectrum.

### Charge Traps

There are about 30 macroscopic charge transfer traps, where as little as 20% of the electrons are transferred during each time step during the readout. These defects result in *bad pixels*, or in the worst cases, *bad columns* and should not be confused with microscopic charge traps which are believed to be the cause of the CTE problem. The traps result in dark tails just above the bad pixel, and bright tails for objects farther above the bad pixel that get clocked out through the defect during the readout. The tails can cause large errors in photometric and astrometric

measurements. In a random field, about 1 out of 100 stars are likely to be affected. Using a program which interpolates over bad pixels or columns (e.g., **wfixup** or **fixpix**) to make a cosmetically better image can result in very large (e.g., tenths of magnitude) errors in the photometry in these rare cases. See also “Charge Traps” on page 26-22.

### Exposure Times: Serial Clocks

The serial clocks option (i.e., the optional parameter `CLOCKS = YES` in the Phase II proposal instructions) is occasionally useful when an extremely bright star is in the field of view, in order to minimize the effects of bleeding. However, when using this option, the shutter open time can have errors of up to 0.25 second. The error in the exposure time occurs as a result of the manner in which the shutters are opened when `CLOCKS=YES` is specified. Header information can be used to correct this error. If the keyword `SERIALS = ON` is in the image header, then the serial clocks were employed. The error in the exposure time depends on the `SHUTTER` keyword. If the value of this keyword is “A”, then the true exposure time is 0.125 second less than that given in the header. If instead the value is “B”, then the true exposure time is 0.25 second less than the header value.

Users should also note that exposure times of non-integral lengths in seconds cannot be performed with the serial clocks on. Therefore, if a non-integral exposure time is specified in the proposal, it will be rounded to the nearest second. The header keywords will properly reflect this rounding, although the actual exposure time will still be short as discussed above.

## 28.2.4 An Example of Photometry with WFPC2

This example shows the steps involved in measuring the magnitude of the star #1461 (Harris et al., 1993) in the Cousins I passband. The image used for this example can be obtained from the HST Archive, or from the WWW at:

[http://www.stsci.edu/ftp/instrument\\_news/WFPC2/Wfpc2\\_phot](http://www.stsci.edu/ftp/instrument_news/WFPC2/Wfpc2_phot)

This WWW directory contains the materials for *WFPC2 ISR 95-04, A Demonstration Analysis Script for Performing Aperture Photometry*. Table 28.5 shows the results from an analysis script similar to *WFPC2 ISR 95-04*, but including some of the corrections discussed above.

```
Images: u2g40o09t.c0h[1] and u2g40o0at.c0h[1]
Position: (315.37,191.16)
Filter: F814W
Exposure Time: 14 seconds
Date of observation: MJD - 49763.4
```

**Table 28.5:** Magnitude of Star #1461 in  $\omega$  Cen

Value	Description
2113.49 counts	Raw counts in 0.5" radius aperture (11 pixels for PC)
-48.63 = 2064.86 counts	Background subtraction (0.12779 counts x 380.522 pix obtained from a 40-pixel radius aperture with an annulus of 5 pixels)
x 0.9915 = 2047.31 counts	Correction for geometric distortion. Not needed if doing surface photometry.
=> 15.481 mag	Raw magnitude ( $= -2.5 \times \log_{10}(2047.31 / 14 \text{ sec}) + 20.894$ ) NOTE: $-2.5 \times \log_{10}(1.987)$ has been added to the zeropoint from Table 28.1 (i.e., 21.639), since these calibrations were taken using the gain=14 setup. Most science observations use gain=7.
-0.10 = 15.381 mag	Aperture correction estimated from Holtzman (1995a).
-0.028 = 15.353 mag	CTE correction (using formulas 1, 2d, 3d from <i>WFPC2 ISR</i> 97-08 with this data)
-0.000 => $m_{F814W} = 15.353$ mag	Contamination correction ( $0.000 \times [49763.4 - 49760.1]$ )
-0.013 => $m_I = 15.340$ mag	Transformation to Cousins I passband

## 28.3 Polarimetry

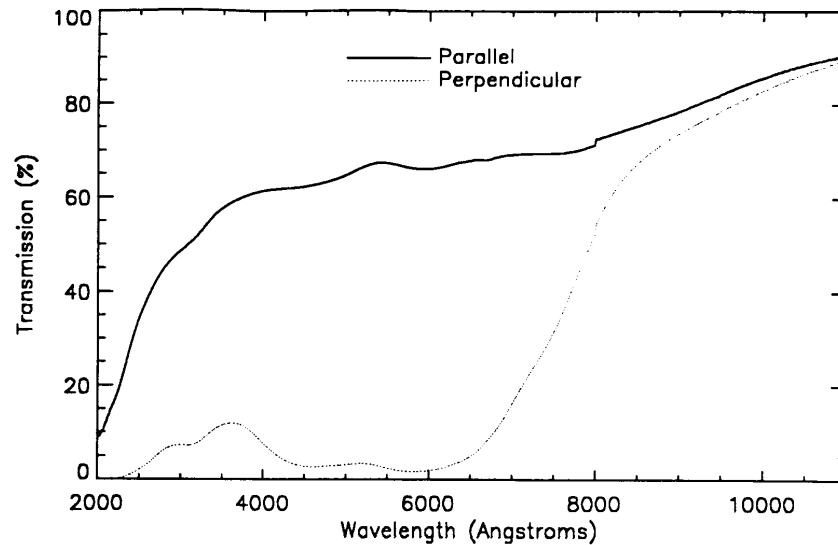
WFPC2 has a polarizer filter which can be used for wide-field polarimetric imaging from about 200 through 700 nm. This filter is a *quad*, meaning that it consists of four panes, each with the polarization angle oriented in a different direction, in steps of  $45^\circ$ . The panes are aligned with the edges of the pyramid, thus each pane corresponds to a chip. However, because the filters are at some distance from the focal plane, there is significant vignetting and cross-talk at the edges of each chip. The area free from vignetting and cross-talk is about 60" square in each WF chip, and 15" square in the PC. It is also possible to use the polarizer in a partially rotated configuration, which gives additional polarization angles at the expense of more severe vignetting.

Each polarimetry observation consists of several images of the same object with different orientations of the polarizer angle. A minimum of three observations is required to obtain full polarimetry information. This can be achieved by observing the target in different chips, by rotating the filter wheel (partial rotation), or by changing the orientation of the HST field of view in the sky, using a different roll angle. In the latter case, observations must frequently occur at different times, as the solar array constraints on HST allow only a limited range of roll angles at any given time.

Accurate calibration of WFPC2 polarimetric data is rather complex, due to the design of both the polarizer filter and the instrument itself. WFPC2 has an

aluminized pick-off mirror with a  $47^\circ$  angle of incidence, which rotates the polarization angle of the incoming light, as well as introducing a spurious polarization of up to 5%. Thus, both the HST roll angle and the polarization angle must be taken into account. In addition, the polarizer coating on the filter has significant transmission of the perpendicular component, with a strong wavelength dependence (see Figure 28.1).

**Figure 28.1:** Parallel and Perpendicular Transmission of the WFPC2 Polarizer



Biretta and McMaster (*WFPC2 ISR 97-11*) recently achieved a calibration accuracy of about 2% rms for well-exposed WFPC2 polarimetry data. Their method uses a Mueller matrix approach to account for the orientation of both telescope and polarizer, the effect of the pick-off mirror, and the significant perpendicular transmission of the polarizer itself. A full description of the motivation behind this approach, the implementation details, and the necessary caveats are given in this document. A web-based tool to aid in the calibration of polarization data has also been developed. With the aid of this tool, polarization properties can be derived for point sources and extended sources from an arbitrary combination of polarized images. The tool is available at:

[http://www.stsci.edu/ftp/instrument\\_news/WFPC2/Wfpc2\\_pol/wfpc2-pol2.html](http://www.stsci.edu/ftp/instrument_news/WFPC2/Wfpc2_pol/wfpc2-pol2.html)

The procedure to obtain polarization information begins with the calibrated images, as they come out of the pipeline (plus cosmic ray and warm pixel rejection, if appropriate). The characteristics of the polarized images and the fluxes in each image are entered in the Web tool, and the calculation started. The tool then reports the values of the Stokes parameters  $I$ ,  $Q$ , and  $U$ , as well as fractional polarization and position angle. The optional **synphot** values in the first part of the tool can be used to fine-tune the results to a specific spectral energy distribution, but are in most cases not necessary.

The tool also reports expressions for  $I$ ,  $Q$ , and  $U$  as a function of fluxes in the three images. These can be used to test the sensitivity of the results to errors in the

individual fluxes, or to combine images in order to obtain pixel-by-pixel values of the Stokes parameters for extended objects, resulting in I, Q, and U images.

More details will be provided in a future ISR, as well as in the extensive help available in the web tool itself.

---

## 28.4 Astrometry

Astrometry with WFPC2 means primarily *relative* astrometry. The high angular resolution and sensitivity of WFPC2 makes it possible, in principle, to measure precise positions of faint features with respect to other reference points in the WFPC2 field of view. On the other hand, the absolute astrometry that can be obtained from WFPC2 images is limited by the positions of the guide stars, usually known to about 0."5 rms in each coordinate, and by the transformation between the FGS and the WFPC2, which introduces errors of order of 0."1 (see *Instrument Science Report OSG-006*).

Because WFPC2 consists of four physically separate detectors, it is necessary to define a coordinate system that includes all four detectors. For convenience, sky coordinates (right ascension and declination) are often used; in this case, they must be computed and carried to a precision of a few mas, in order to maintain the precision with which the relative positions and scales of the WFPC2 detectors are known. It is important to remember that the coordinates are *not* known with this accuracy. The absolute accuracy of the positions obtained from WFPC2 images is typically 0."5 rms in each coordinate and is limited primarily by the accuracy of the guide star positions.

The recommended way to convert pixel coordinates into relative coordinates is to use the task **metric**, which can handle both WF/PC and WFPC2 images. For WFPC2 images, **metric** corrects for the *geometric distortion* introduced by the camera optics, primarily the field flattening lenses, and brings the four chips into the *metachip* reference system, defined so as to have the same orientation and plate scale as the WF2 chip at its center. These coordinates are then converted into right ascension and declination by using the position and orientation of the WF2 chip. A related task, **invmetric**, can be used to effect the opposite transformation, from right ascension and declination to chip and pixel position. The final relative positions are accurate to better than 0."005 for targets contained on one chip, and 0."1 for targets on different chips. Note that both **metric** and **invmetric** include specialized information about the geometry of WFPC2. They do *not* use the header parameters that describe the world coordinate system (CRVAL1 and 2, CRPIX1 and 2, and the CDMATRIX) to relate positions in different chips. Of these parameters, only the values for WF2 are used to convert the metachip positions to and from right ascension and declination. As a side effect, neither task can work on images that do not contain WF2, for which the **xy2rd** task can be used.

Early WFPC2 images contain header parameters with less accurate values of the plate scale and of the chip-to-chip rotations. The task **uchcoord** will modify

the header parameters of these images to reflect more current information. The task **uchcoord** also corrects the header parameters for an error that occurred between April 11 and 19, 1994. The task will stamp the file after the transformation, to prevent users from unwittingly correcting the same image twice. It is recommended that **uchcoord** be run on all images taken before March 1995; the task will not apply any correction unless it is warranted, and thus it is safe to run on any WFPC2 image. There is also some evidence, both from internal exposures and from a study of many external WFPC2 exposures taken over the years (Ratnatunga et al., 1997), that the relative position of the four detectors may have shifted by up to 0."1 since launch, and especially across the cooldown of April 23, 1994. A regular monitoring program (CAL 7627) is in place to follow such variations. Should they occur again, the relevant tasks, **metric** and **invmetric**, will be modified to return the information appropriate to the date of observation.

Rough coordinates can also be obtained using the task **xy2rd**, which uses the world coordinate system parameters in each group to determine the coordinates associated with a given pixel position. However, **xy2rd** does not use the most recent information on the relative chip positions, and it does not apply the geometric correction. Each can result in an error of about 0."3, especially near the edges of the chip; typical errors are closer to 0."1.

---

## 28.5 Dithering

The pixels of the PC undersample the point spread function (PSF) of the HST by a factor of about two, and the pixels of the WF are a factor of two coarser yet. Thus WFPC2 does not recover a substantial fraction of the spatial information that exists at the focal plane of the instrument. However, this information is not completely lost. Some of it can be recovered by *dithering* or *sub-stepping* the position of the chips by non-integral pixel amounts.

The recovery of high frequency spatial information is fundamentally limited by the pixel response function (PRF). The PRF of an ideal CCD with square pixels is simply a square boxcar function the size of the pixel. In practice, the PRF is a function not only of the physical size of the pixels, but also the degree to which photons and electrons are scattered into adjacent pixels, as well as smearing introduced by telescopic position wandering. The image recorded by the CCD is the "true" image (that which would be captured by an ideal detector at the focal plane) convolved with this PRF. Thus, at best, the image will be no sharper than that allowed by an ideal square pixel. In the case of WFPC2, in which at least 20% of the light falling on a given pixel is detected in adjacent pixels, the image is even less sharp.

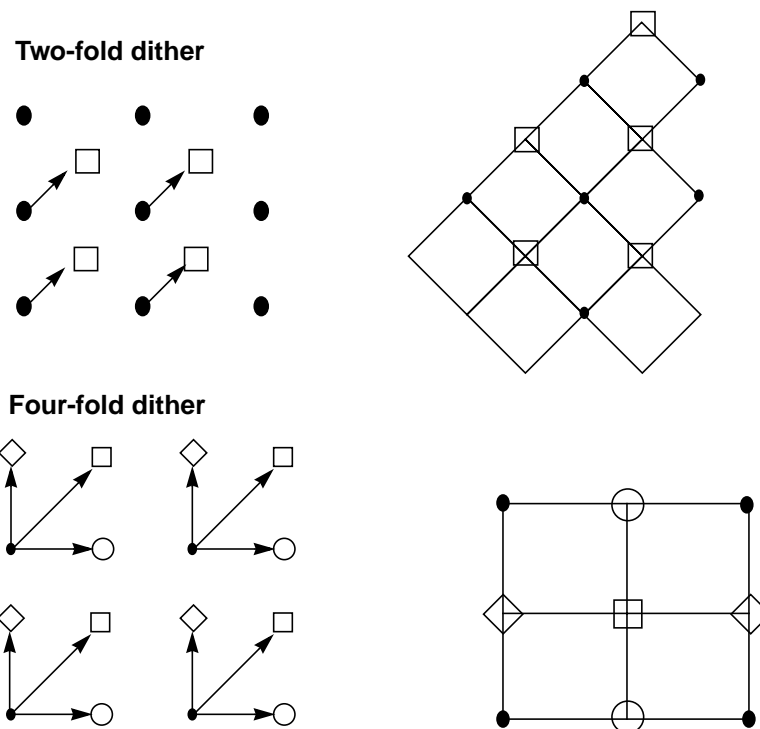
The PRF of an ideal square pixel, that is a boxcar function, severely suppresses power on scales comparable to the size of the pixel. According to the Shannon-Nyquist theorem of information theory the sampling interval required to capture nearly all of the information passed by square pixels is 1/2 the size  $l$  of a pixel. This corresponds to dithering the CCD from its starting position of (0,0) to

three other positions,  $(0, 1/2 l)$ ,  $(1/2 l, 0)$  and  $(1/2 l, 1/2 l)$ ; however, in practice, much of the information can be regained by a single dither to  $(1/2 l, 1/2 l)$ .

The process of retrieving high-spatial resolution information from dithered images can be thought of as having two stages. The first, reconstruction, removes the effect of sampling and restores the image to that produced by the convolution of the PSF and PRF of the telescope and detector. The more demanding stage, deconvolution (sometimes called restoration), attempts to remove much of the blurring produced by the optics and detector. In effect, deconvolution boosts the relative strength of the high-frequency components of the Fourier spectrum to undo the suppression produced by the PSF and PRF.

If your observations were taken with either of the two dither patterns discussed above, and if the positioning of the telescope was accurate to about a tenth of a pixel (this is usually but not always the case), then you can reconstruct the image merely by interlacing the pixels of the offset images. In the case of a two-fold dither—that is images offset by a vector  $(n + 1/2, n + 1/2)$  pixels, where  $n$  is an integer—the interlaced images can be put on a square grid rotated  $45^\circ$  from the original orientation of the CCD (see Figure 28.2, top). In the case of a four-fold dither, the images are interlaced on a grid twice as fine as the original CCD and coaligned with it (see Figure 28.2, bottom).

**Figure 28.2:** Interlacing Pixels of Offset Images



As part of the Hubble Deep Field project, a new method was developed to linearly reconstruct multiple offset images. This method, variable pixel linear reconstruction (also known as *drizzle*), can be thought of as shifting and adding with a variable pixel size. For poorly sampled data, the shifted pixels retain the

initial pixel size—the final image combines the shifts correctly, but the gain in resolution is minimal. For a well-sampled field, such as that of the Hubble Deep Field, the size of the shifted pixels can be made quite small, and the image combination becomes equivalent to interlacing. Drizzling also corrects for the effects of the geometric distortion of WFPC2; correction of geometric distortion is important if shifts between dithered images are of order ten pixels or more.

The drizzle algorithm was implemented as the STSDAS task **drizzle**, as part of the **dither** package, which helps users combine dithered images. The **dither** package is included in STSDAS release v2.0.1 and later, and includes the following tasks:

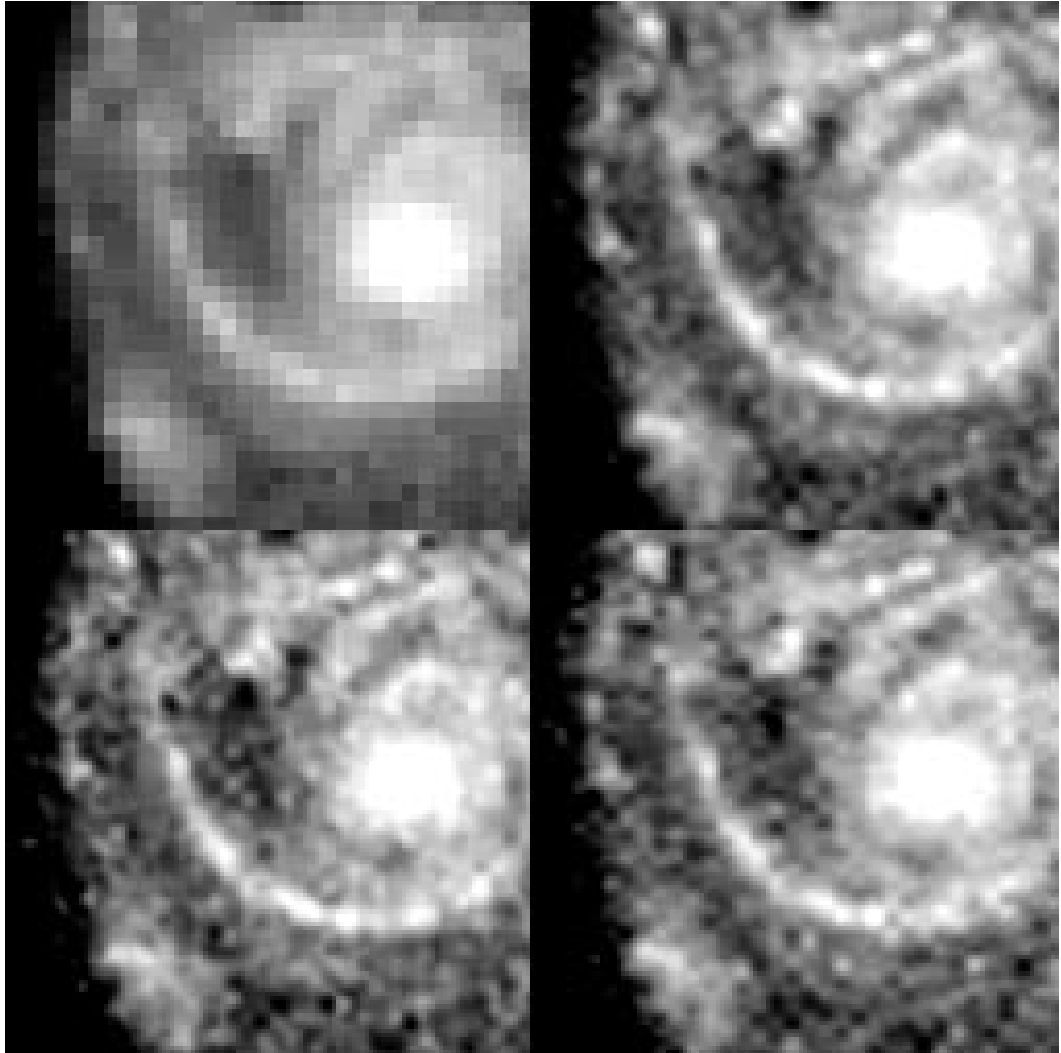
- **precor**: Determines regions of the image containing astrophysical objects and nulls the remainder of the image, substantially reducing the effect of cosmic rays and chip defects on the offset measurement. The output from **precor** is only used for offset determination and not final image creation.
- **offset**: Cross-correlates all four images in a WFPC image, creating output cross-correlation images with names that can be appropriately grouped by later tasks. Uses the task **crossdriz** to perform the cross-correlation.
- **crossdriz**: Cross-correlates two images, after preprocessing which includes trimming, and, if requested, drizzling to remove geometric distortion or rotation. **crossdriz** will also perform a loop over a range of test rotation angles.
- **shiftfind**: Locates the peak in a cross-correlation image and fits for sub-pixel shift information. The search region and details of the fitting can be adjusted by the user.
- **rotfind**: Fits for the rotation angle between two images. **rotfind** is called when **crossdriz** has been used to loop over a range of test rotation angles between two images.
- **avshift**: Determines the shifts between two WFPC2 images by averaging the results obtained on each of the groups after adjusting for the rotation angles between the four groups. **avshift** can also be used to estimate the rotation angle between two different WFPC2 images, when the rotation angle is a small fraction of a degree.
- **blot**: Maps a drizzled image back onto an input image. This is an essential part of the tasks we are developing for removing cosmic rays from singly-dithered images.

Additional information on these tasks is available in Fruchter et al. (1997) and Mutchler and Fruchter (1997), as well as the on-line help files.

Although reconstruction largely removes the effects of sampling on the image, it does not restore the information lost to the smearing of the PSF and PRF. Deconvolution of the images, however, does hold out the possibility of recapturing much of this information. Figure 28.3, supplied by Richard Hook of the ST-ECF, shows the result of applying the Richardson-Lucy deconvolution scheme to HST data, used extensively in the analysis of WF/PC-1 data. The upper-left image shows one of four input images. The upper-right image shows a

deconvolution of all of the data, and the lower two images show deconvolutions of independent subsets of the data. A dramatic gain in resolution is evident.

**Figure 28.3:** Richardson-Lucy Deconvolution of HST Data



A version of the Richardson-Lucy (RL) deconvolution scheme capable of handling dithered WFPC2 data is already available to STSDAS users. It is the task **acoadd** in the package **stsdas.contrib**. In order to use **acoadd**, users will need to supply the program both with a PSF (which in practice should be the convolution of the PRF with the optical PSF) and with the offsets in position between the various images. The position offset between the two images can be obtained using the task **crossdriz** in the **dither** package.

In principle, image deconvolution requires an accurate knowledge of both the instrument PSF and PRF. At present, our best models of the WFPC2 PSF come from the publicly available TinyTim software (Krist, 1995). The quality of the TinyTim model can be improved substantially by taking into account the exact position of the source within the pixel. Remy et al. (1997) discuss how this can be

accomplished by generating multiple TinyTim images at various focus and jitter values, oversampled with respect to the camera pixels. At present, this is very labor-intensive, and the results cannot be easily integrated into the existing deconvolution software. Another limitation of the existing software is that it cannot incorporate the significant variation of the PSF across the field of view. As a result, the Richardson-Lucy approach can only be applied to limited regions of a chip at a time. Nonetheless, tests done on WFPC2 images suggest that RL deconvolution can give the WFPC2 user a substantial gain in resolution even in the presence of typical PSF and PRF errors. Users interested in more information on dithering, reconstruction, and deconvolution should consult the February and September 1995 issues of the ST-ECF Newsletter, where these issues are discussed in detail.

---

## 28.6 Accuracy of WFPC2 Results

Table 28.6 summarizes the accuracy to be expected from WFPC2 observations in several areas. The numbers in the table should be used with care, and only after reading the relevant sections of this handbook and the documents referenced therein; they are presented in tabular form here for easy reference.

**Table 28.6:** Accuracy Expected in WFPC2 Observations

Procedure	Estimated Accuracy	Notes
<i>Calibration (flatfielding, bias subtraction, dark correction)</i>		
Bias subtraction	0.1 DN rms	Unless bias jump is present
Dark subtraction	0.1 DN/hr rms	Error larger for warm pixels; absolute error uncertain because of dark glow
Flatfielding	<1% rms large scale	Visible, near UV
	0.3% rms small scale	
	~10%	F160BW; uncertain
<i>Relative photometry</i>		
Residuals in CTE correction	< 1% rms (above 1000 DN)	
	3% rms (at 100 DN)	
Long vs. short anomaly (uncorrected)	< 1% rms (above 10000 DN)	
	5% (at 1000 DN)	
	15% (at 100 DN)	
Aperture correction	4% rms focus dependence (1 pixel aperture)	Can (should) be determined from data
	<1% focus dependence (> 5 pixel)	
	1-2% field dependence (1 pixel aperture)	
Contamination correction	3% rms max (28 days after decon) (F160BW)	
	1% rms max (28 days after decon) (filters bluer than F555W)	
Background determination	0.1 DN/pixel (background > 10 DN/pixel)	May be difficult to exceed, regardless of image S/N
Pixel centering	< 1%	
<i>Absolute photometry</i>		
Sensitivity	< 2% rms for standard photometric filters	Red leaks are uncertain by ~10%
	2% rms for broad and intermediate filters in visible	
	< 5% rms for narrow-band filters in visible	
	2-8% rms for UV filters	
<i>Astrometry</i>		
Relative	0.005" rms (after geometric correction)	Same chip
	0.1" (estimated)	Across chips
Absolute	1" rms (estimated)	

---

## 28.7 References

- Casertano, S., 1998, in *The 1997 HST Calibration Workshop*, eds. S. Casertano et al., (Baltimore: Space Telescope Science Institute), in press.
- Fruchter, A.S., et al., in *The 1997 HST Calibration Workshop*, eds. S. Casertano et al., (Baltimore: Space Telescope Science Institute), in press.
- Harris, H.C., et al., 1993, *AJ*, 105, 1196.
- Holtzman, J.A., et al., 1995a, *PASP*, 107, 156.
- Holtzman, J.A., et al., 1995b, *PASP*, 107, 1065.
- Krist, J., 1995, "Simulation of HST PSF Using TinyTim," in *Astronomical Data Analysis, Software, and Systems IV*, Shaw et al., eds. (San Francisco: Astronomical Society of the Pacific), p. 349.
- Mutchler, M., and A. Fruchter, 1998, in *The 1997 HST Calibration Workshop*, eds. S. Casertano et al., (Baltimore: Space Telescope Science Institute), in press.
- Oke, J.B., 1974, *ApJS*, 27, 21.
- Ratnatunga, K.U., et al., 1998, in *The 1997 HST Calibration Workshop*, eds. S. Casertano et al., (Baltimore: Space Telescope Science Institute), in press.
- Remy, M., et al., 1998, in *The 1997 HST Calibration Workshop*, eds. S. Casertano et al., (Baltimore: Space Telescope Science Institute), in press.
- Surdej, J., et al., 1998, in *The 1997 HST Calibration Workshop*, eds. S. Casertano et al., (Baltimore: Space Telescope Science Institute), in press.
- Trauger, J.T., et al., 1994, *ApJ*, 435, L3.
- Trauger, J.T., 1998, in *The 1997 HST Calibration Workshop*, eds. S. Casertano et al., (Baltimore: Space Telescope Science Institute), in press.
- Wiggs, M.S., et al., 1998, in *The 1997 HST Calibration Workshop*, eds. S. Casertano et al., (Baltimore: Space Telescope Science Institute), in press.

